People`s Democratic Republic of Algeria

Ministry of Higher Education and Scientific Research

University of Echahid Hamma Lakhdar - El oued Faculty of Technology

Department of Process Engineering and Petrochemicals

Dissertation

ACADEMIC MASTER

Domain: Science and Technology

Division: Process Engineering

Specialty: Chemical Engineering

Presented by:

1. Chaima Tedjini
2. Aya othmani

Entitled:

In Silico Repurposing of Pioglitazone as an Inhibitor of Cancer-Associated Hexokinase II

Dissertation Submitted in Partial Fulfillment of the Requirements for the Master Degree in Chemical Engineering

Publicly defended in: 24 /05 /2026

Board of Examiners:

Ms. Lami Nassima	Associate Professor	University of El-Oued	Chairman
Ms. Mohammed Laid Tedjani	Associate Professor	University of El-Oued	Examiner
Ms. Benamara Hacen	Associate Professor	University of El-Oued	Supervisor

Academic Year: 2025/2026

Dedication

"**And whoever said we were not worthy of it? We attained it, despite all odds**"

The journey was neither short nor easy, but we did it... we achieved it.

All praise is due to Allah, first and last, who granted us success.

We dedicate this achievement to our beloved fathers, who never clipped our wings and taught us resilience, and to our dear mothers, whose endless prayers and tender hearts paved our way. You are the source of our strength. 2.

To our families and friends, thank you for being our unwavering support, our light in difficult days, and for sharing every moment of exhaustion and joy.

To each other, as partners in this long journey, thank you for being a sister, a friend, and a constant blessing every step of the way.

And finally, praise be to God, first and last, and praise be to God in all circumstances.

 # Chaima &Aya

Acknowledgments

First and foremost, all praise is due to Allah, and peace and blessings be upon our Master Muhammad, his family, and his companions.

We would like to express our profound gratitude to our respected supervisor, **Dr. Hacen Benamara**, for his invaluable guidance, continuous support, and extensive expertise throughout the development of this thesis. His insightful recommendations and unwavering encouragement were instrumental in the completion of this work. May Allah bless him and reward him abundantly for his dedication and generosity.

Lastly, we are deeply indebted to our families and to all those who provided us with encouragement, assistance, and support throughout this journey. Their confidence in us has been a source of motivation and perseverance.

Abstract

Cancer cells undergo a metabolic shift (the Warburg effect) that prioritizes rapid glycolysis over oxidative phosphorylation, heavily driven by the overexpression of Hexokinase II (HKII) anchored to the outer mitochondrial membrane. Because de novo drug development is resource-intensive, drug repurposing offers an accelerated therapeutic alternative. Pioglitazone, an approved anti-diabetic thiazolidinedione, exhibits off-target anti-cancer properties by directly interacting with mitoNEET (CISD1), an outer mitochondrial iron-sulfur [2Fe-2S] cluster protein essential for cellular bioenergetics.

This study uses integrated *in silico* computational approaches to evaluate the potential of pioglitazone as an indirect metabolic inhibitor of cancer-associated HKII via mitoNEET targeting.

The 3D crystal structure of human mitoNEET (PDB ID: 6DE9) was prepared and subjected to site-directed molecular docking simulations using AutoDock Vina, with protocol accuracy validated at an RMSD threshold of 1.896 Å. Computational outcomes were comparatively benchmarked against Furosemide, a known mitoNEET modulator. Pharmacoinformatics (*in silico* ADME) and acute systemic safety profiles were mapped via SwissADME and ProTox-3.0 pipelines.

Pioglitazone demonstrated a high target affinity for the mitoNEET regulatory domain with a highly favorable Gibbs free energy score ($\Delta G = -31.8$ kJ/mol; binding constant 3.7×10^5), substantially outperforming Furosemide ($\Delta G = -26.4$ kJ/mol; binding constant 4.2×10^4). ADME screening confirmed strong drug-likeness, passive membrane permeability, and optimal lipophilicity ($\log P = 3.49$). Toxicological profiling classified pioglitazone under a safe acute operational envelope (Toxicity Class 4; $LD_{50} = 1000$ mg/kg), with low cardiotoxic or stress-response risks, though monitoring for potential hepatotoxicity (probability 0.70) remains necessary.

This research establishes a solid molecular foundation for repurposing pioglitazone in computational oncology. By binding stably to mitoNEET, pioglitazone is structurally positioned to alter mitochondrial bioenergetics and disrupt the vital ATP supply required for HKII-mediated cancer survival, justifying further advancement to *in vitro* validation assays.

Keywords: Drug Repurposing, Pioglitazone, Hexokinase II, MitoNEET (CISD1), Molecular Docking, Cancer Metabolism.

الملخص

تخضع الخلايا السرطانية لتحول استقلابي (تأثير واربورغ - Warburg effect) يعطي الأولوية لتحلل الجلوكوز السريع على الفسفرة التأكسدية، وهو أمر مدفوع بشكل كبير بالتعبير المفرط لإنزيم الهيكسوكيناز الثاني (HKII) المرتبط بالغشاء الميتوكوندري الخارجي. ونظرًا لأن تطوير الأدوية من الصفر يتطلب موارد كثيفة، فإن إعادة توجيه الأدوية (Drug repurposing) تقدم بديلًا علاجيًا متسارعًا.

يُظهر عقار "بيوجليتارون" (Pioglitazone)، وهو دواء معتمد من فئة "الثيازوليدينديون" لمكافحة مرض السكري، خصائص مضادة للسرطان خارج الهدف من خلال التفاعل المباشر مع بروتين "ميتونيت" (mitoNEET / CISD1)، وهو بروتين حديد-كبريت [2Fe-2S] متواجد في الغشاء الميتوكوندري الخارجي ويعد أساسيًا للطاقة الحيوية الخلوية.

تستخدم هذه الدراسة مناهج حاسوبية متكاملة داخل المحاكاة (in silico) لتقييم إمكانات البيوجليتازون كمثبط استقلابي غير مباشر لإنزيم HKII المرتبط بالسرطان عبر استهداف بروتين ميتونيت. تم تحضير البنية البلورية ثلاثية الأبعاد لبروتين ميتونيت البشري (PDB ID: 6DE9) وإخضاعها لمحاكاة الالتحام الجزيئي الموجه للموقع باستخدام برنامج (AutoDock Vina)، حيث تم التحقق من دقة البروتوكول عند عتبة جذر متوسط مربع الانحراف (RMSD) بلغت 1.896 أنجستروم.

تمت مقارنة النتائج الحاسوبية مرجعيًا مع عقار "فوروسيميد" (Furosemide)، وهو منسق معروف لبروتين ميتونيت. كما تم رسم خرائط المعلوماتية الدوائية (ADME داخل المحاكاة) وملفات السلامة الجهازية الحادة عبر منصتي (SwissADME) و (ProTox-3.0).

أظهر البيوجليتازون ألفة ارتباط عالية بالنطاق التنظيمي لبروتين ميتونيت مع درجة طاقة جيبس الحرة مواتية للغاية ($\Delta G = -31.8$ kJ/mol) ؛ وثابت ارتباط بلغ ($k_b = 3.7 \times 10^5$)، متفوقًا بشكل كبير على الفوروسيميد ($\Delta G = -26.4$ kJ/mol) ؛ وثابت ارتباط بلغ ($k_b = 4.2 \times 10^4$). وأكد فحص (ADME) الخصائص القوية الشبيهة بالدواء، والنفاذية السلبية للغشاء، ودرجة ذوبان مثالية في الدهون (log P = 3.49).

صنف التوصيف السمي البيوجليتازون ضمن غلاف تشغيلي حاد وآمن (فئة السمية 4؛ الجرعة المميتة النصفية LD_{50} = 1000 mg/kg)، مع مخاطر منخفضة للاستجابة للإجهاد أو السمية القلبية، على الرغم من أن مراقبة السمية الكبدية المحتملة (بإحتمالية 0.70) تظل ضرورية.

يؤسس هذا البحث لركيزة جزيئية صلبة لإعادة توجيه عقار البيوجليتازون في مجال أورام السرطان الحاسوبية. فمن خلال الارتباط المستقر ببروتين ميتونيت، يتمتع البيوجليتازون بموقع بنيوي يسمح له بتعديل الطاقة الحيوية للميتوكوندريا وتعطيل إمدادات الطاقة (ATP) الحيوية اللازمة لبقاء الخلايا السرطانية المعتمدة على إنزيم HKII، مما يبرر تقدمه إلى اختبارات التحقق المخبرية (in vitro).

الكلمات المفتاحية:

إعادة توجيه الأدوية، بيوجليتازون، هيكسوكيناز الثاني (HKII)، ميتونيت (CISD1)، الالتحام الجزيئي، استقلاب السرطان.

Table of Contents

Chapter II

Chapter III

Chapter IV

List of figures

List of tables

List of Abbreviations and Symbols

Abbreviation	Meaning
ADME	Absorption, Distribution, Metabolism, and Excretion
ANT	Adenine Nucleotide Transporter (also referred to as Adenine Nucleotide Translocase)
ATP	Adenosine Triphosphate
Cys	Cysteine
CISD1	CDGSH Iron Sulfur Domain 1 (Alternative name for mitoNEET)
ESP	Electrostatic Potential
FES	Iron-Sulfur Cluster identifier / tag
FhMM	outer Mitochondrial Membrane fold/region label *(from anatomical diagrams)*
G6P (or **Glu-6-P**)	Glucose-6-Phosphate
His	Histidine
HKII	Hexokinase II
IMM	Inner Mitochondrial Membrane
IMS	Intermembrane Space
LD50	Lethal Dose, 50% (Median Lethal Dose)
Lys	Lysine
NADPH	Nicotinamide Adenine Dinucleotide Phosphate (Reduced)
oMM	outer Mitochondrial Membrane
oXPHoS	oxidative Phosphorylation
PDB	Protein Data Bank
PEP	Phosphoenolpyruvate
PPARγ	Peroxisome Proliferator-Activated Receptor Gamma
SBDD	Structure-Based Drug Design
SMILES	Simplified Molecular-Input Line-Entry System
TCA	Tricarboxylic Acid Cycle (Krebs Cycle)

TPSA	Topological Polar Surface Area
TZD	Thiazolidinedione
VDAC	Voltage-Dependent Anion Channel

General Introduction

Cancer cells exhibit a profound metabolic reprogramming known as the Warburg effect, a phenomenon where they selectively prioritize high-rate aerobic glycolysis over oxidative phosphorylation to fuel their rapid growth and survival, even in oxygen-abundant environments [1]. A pivotal driver and gatekeeper of this reprogrammed fuel supply is Hexokinase II (HKII), an enzyme frequently overexpressed in malignant phenotypes [2]. In cancer cells, HKII undergoes a spatial relocation to the outer mitochondrial membrane, physically coupling with the Voltage-Dependent Anion Channel (VDAC). This strategic localization grants HKII immediate access to newly synthesized mitochondrial ATP, drastically accelerating glycolytic flux, providing necessary carbon skeletons for biomass synthesis, and actively suppressing pro-apoptotic signals to grant significant chemotherapeutic resistance [3].

Because the de novo design of novel oncological therapeutics is an exceedingly long, financially intensive, and high-risk process, the biomedical community has increasingly turned toward therapeutic drug repurposing. Drug repositioning leverages the established safety profiles of clinically approved medications, thereby accelerating translational timelines and delivering treatments to patients more efficiently. This thesis utilizes advanced *in silico* computational modeling and pharmacoinformatics profiling to investigate the structural feasibility of repurposing Pioglitazone a well-established thiazolidinedione (TZD) medication traditionally utilized as a

cornerstone for managing insulin resistance in type 2 diabetes as a targeted metabolic intervention against cancer [4-5].

In addition, preclinical evidence indicates that Pioglitazone exerts pleiotropic, off-target anti-proliferative activities that are independent of insulin signaling, suggesting direct interaction with mitochondrial components. Emerging research identifies the outer mitochondrial membrane protein MitoNEET (CISD1), which acts as an essential sensor for redox balance and iron-sulfur cluster transfer, as a critical player closely linked to Hexokinase II-dependent tumor metabolism. The general objective of this study is to implement site-directed molecular docking and ADME-Tox profiling to evaluate how Pioglitazone interacts within the active pocket of MitoNEET compared to reference standards like Furosemide. Through this integrated computational approach, the research aims to establish a precise molecular basis for exploiting Pioglitazone to disrupt mitochondrial homeostasis, elevate selective oxidative stress, and ultimately impair the energy supply cascades of malignant cells.

Chapter I

Background and objectives of Pioglitazone–Hexokinase II

I.1 Therapeutic Repurposing of Pioglitazone against HKII

Cancer cells undergo a metabolic shift known as the Warburg effect [6], where they prioritize a specific energy production process to support rapid growth. A key driver of this process is an enzyme called Hexokinase II (HKII) [7], which acts as a gatekeeper for the cell's fuel supply. Because creating new drugs is a long and expensive process, researchers are exploring drug repurposing using existing, approved medications for new purposes. This study uses computer modeling to investigate whether Pioglitazone, a common drug for type 2 diabetes, can **indirectly target** and inhibit HKII to disrupt the energy supply of cancer cells [8].

I.2 Chemical Background of Pioglitazone

I.2.1 Molecular Structure and Physicochemical Properties

Pioglitazone, chemically identified as (RS)-5-{4-[2-(5-ethylpyridin-2yl)ethoxy] benzyl} thiazolidine -2,4-dione, possesses a molecular formula of $C_{19}H_{20}N_2O_3S$ and a molecular weight of approximately 356.44 g/mol [9]. The molecule is characterized by a central benzene ring connected to a pyridine ring via an ethoxy bridge on one side, and a **thiazolidinedione (TZD)** scaffold on the other [10].

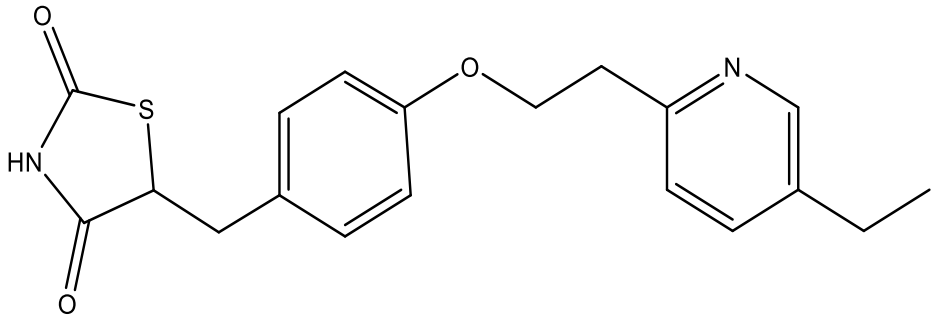

Figure 1: Molecular Structure of Pioglitazone

The TZD moiety is the pharmacophoric core responsible for its primary biological activity [11]. This heterocyclic ring contains two carbonyl groups at positions 2 and 4 and a sulfur atom, which facilitates specific hydrogen-bonding patterns with protein residues [12]. Its physicochemical properties include a logP value of approximately 2.3, indicating moderate lipophilicity, and limited aqueous solubility, which necessitates careful formulation to ensure clinical efficacy [13].

I.3 Therapeutic Applications Beyond Diabetes

While pioglitazone is a cornerstone in managing insulin resistance through PPARγ activation, its pleiotropic effects have sparked interest in oncology [14]. Preclinical models have demonstrated that pioglitazone can modulate cell cycle arrest and induce differentiation in various cancer cell lines [15]. These off-target effects are often independent of PPARγ signaling, suggesting direct interaction with metabolic enzymes or mitochondrial proteins involved in tumor progression [16].

I.4 MitoNEET: Localization and Main Functions in Human Cells

MitoNEET, also known as CISD1, represents the first identified member of the NEET protein family characterized by a unique CDGSH iron-sulfur domain. This small protein plays a critical role in metabolic homeostasis by acting as a sensor for oxidative stress and **regulating iron-sulfur cluster transfer** within the cellular environment [17].

- **Main Biological Role**

The primary function of mitoNEET involves the regulation of mitochondrial bioenergetics and iron signaling. It acts as a redox-sensitive tether that facilitates the transfer of [2Fe-2S] clusters to acceptor proteins, thereby influencing mitochondrial respiration and lipid metabolism [18]. By modulating the iron content within the mitochondrial matrix, mitoNEET prevents the accumulation of toxic reactive oxygen species and maintains the functional integrity of the electron transport chain [19].

- **Localization in Human Cells**

MitoNEET is predominantly anchored to the outer mitochondrial membrane (OMM) through its N-terminal hydrophobic sequence [20]. Its larger C-terminal domain, which contains the iron-

sulfur binding site, faces the cytosol, allowing it to serve as a molecular bridge between the mitochondria and other cytosolic signaling pathways. Research indicates that this orientation is vital for its interactions with various cytosolic partners and its role in coordinating cellular iron distribution [21].

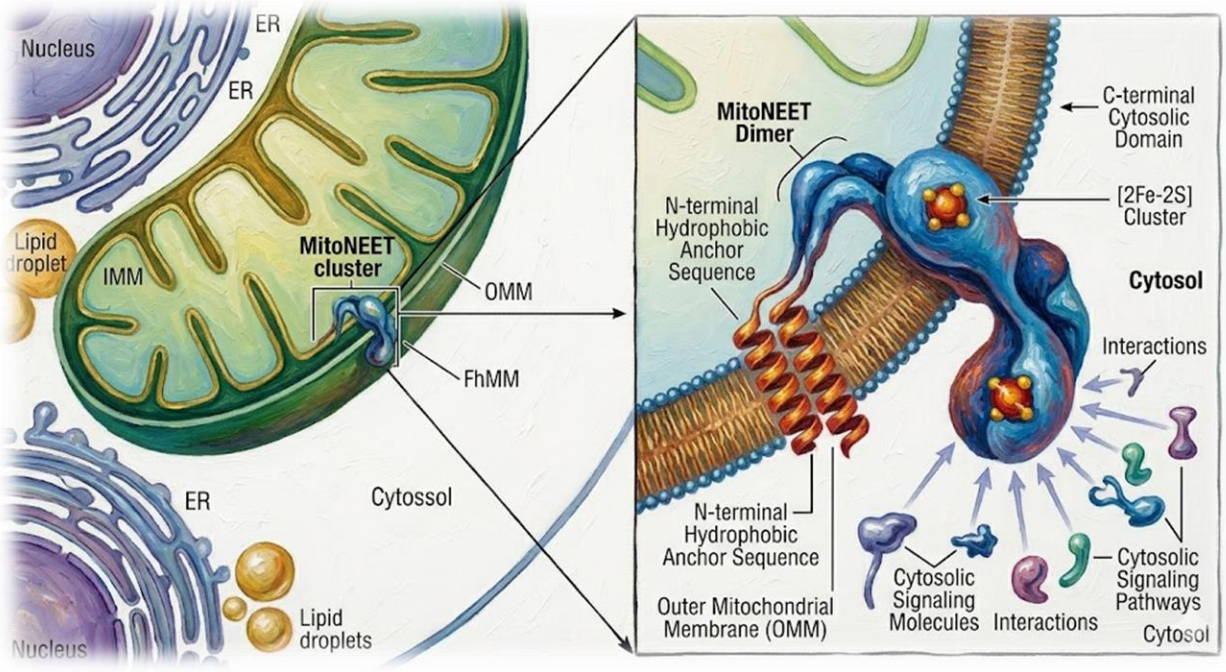

Figure 2: Structural organization and Subcellular Localization of the MitoNEET Protein

I.4.1 Role of Mitochondria in ATP Generation Following mitoNEET Activity

Mitochondria are the primary sites for aerobic respiration, where adenosine triphosphate (ATP) is synthesized through oxidative phosphorylation [22]. The activity of mitoNEET significantly influences this process by controlling the availability of iron-sulfur clusters required for the assembly of complexes I, II, and III, which are essential components of the respiratory chain [23].

I.4.2 Hexokinase II (HKII) in Cancer Pathophysiology: Biological Function and Metabolic Regulation

In malignant phenotypes, **Hexokinase II (HKII)** serves as the primary engine for the **Warburg Effect**. Frequently overexpressed, HKII undergoes a critical spatial relocation to the **outer**

mitochondrial membrane (oMM), where it physically couples with the **Voltage-Dependent Anion Channel (VDAC)** [24].

This strategic anchoring provides HKII with preferential access to mitochondrial **ATP** exported via the **Adenine Nucleotide Transporter (ANT)**, bypassing the limitations of cytosolic diffusion. By tethering glycolysis directly to mitochondrial output, cancer cells achieve:

- **Accelerated Glycolytic Flux:** Rapid conversion of glucose to Glucose-6-Phosphate (Glu-6-P), fueling both the Pentose Phosphate Pathway for biosynthesis and lactate production [25].
- **Metabolic Flexibility:** The ability to sustain high-velocity energy production even in normoxic conditions [26].
- **Apoptotic Resistance:** The HKII-VDAC complex actively suppresses the release of pro-apoptotic factors, granting the cell a significant survival advantage against chemotherapy-induced death [27].

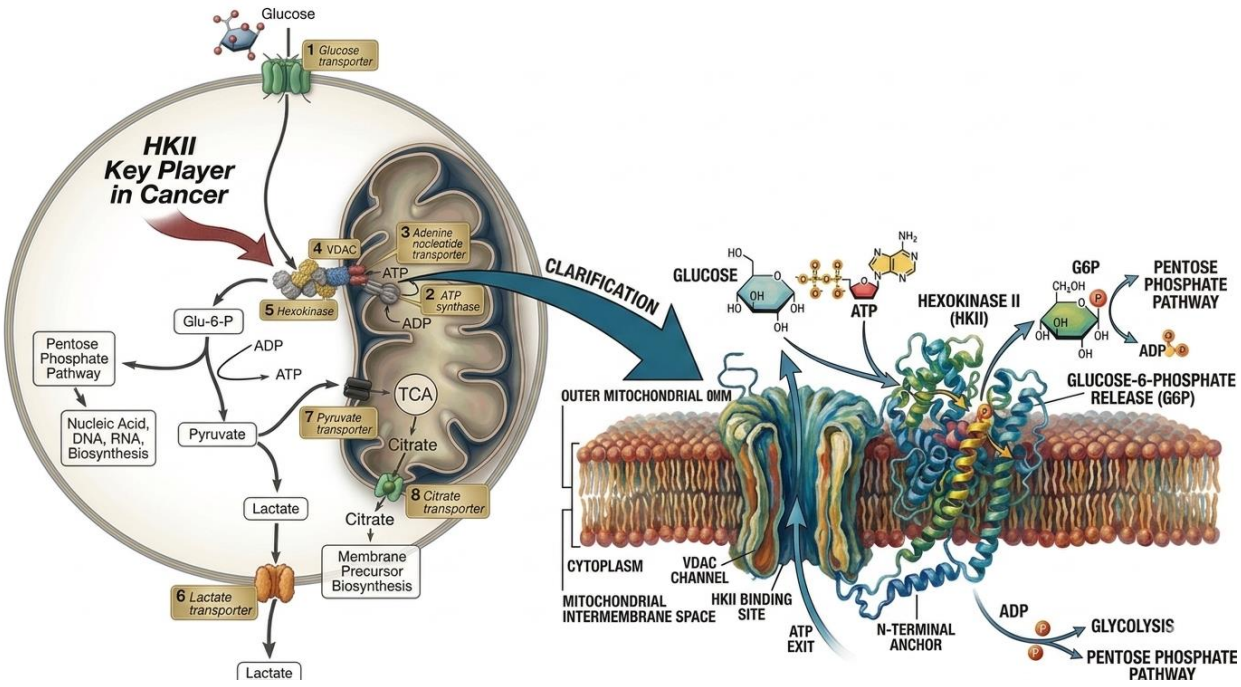

Figure 3: The Role of Mitochondrial-Bound Hexokinase II in Cancer Metabolic Reprogramming

- **Warburg effect**

The Warburg effect describes a metabolic shift in cancer cells, where they prioritize high-rate aerobic glycolysis over oxidative phosphorylation, even in oxygen-rich environments [28]. This phenomenon facilitates rapid ATP production and provides essential carbon skeletons for biosynthetic pathways, supporting the uncontrolled proliferation and survival of malignant tissues [29].

I.4.3 Exploiting Mitochondrial ATP to Increase Hexokinase II Activity

The reactivity of HKII toward Voltage-Dependent Anion Channels (VDACs) on the mitochondrial surface allows the utilization of the ATP exported from the mitochondrial matrix via the adenine nucleotide translocase [30]. By tapping into this local pool of newly synthesized ATP, HKII maintains a high reaction velocity, which effectively bypasses the limitations of lower cytosolic ATP concentrations [31].

I.4.4 Coupling Glucose and ATP via Hexokinase II

The physical coupling of HKII to the mitochondria creates a highly efficient metabolic microenvironment [32]. This arrangement facilitates the immediate transfer of phosphate groups to glucose, minimizing energy dissipation. This tight coupling not only drives the glycolytic pathway forward but also regulates mitochondrial function by modulating the ADP/ATP ratio across the membrane, thus providing a feedback mechanism between cytosolic demand and mitochondrial supply [33].

I.4.5 Glucose Phosphorylation

Glucose phosphorylation is a fundamental biochemical process that ensures the retention of glucose within the cytoplasm and its subsequent entry into metabolic cycles [34]. This process is tightly regulated by the proximity of hexokinases to mitochondrial energy sources, ensuring that the rate of glucose entry matches the energetic requirements of the cell [35].

I.4.6 G6P Generation Utilizing Mitochondrial ATP

The generation of glucose-6-phosphate (G6P) using ATP derived from mitochondria is a strategic metabolic step that determines the fate of carbon atoms within the cell. The localized production of G6P ensures that metabolic intermediates are available for either energy production or the synthesis of essential macromolecules [36].

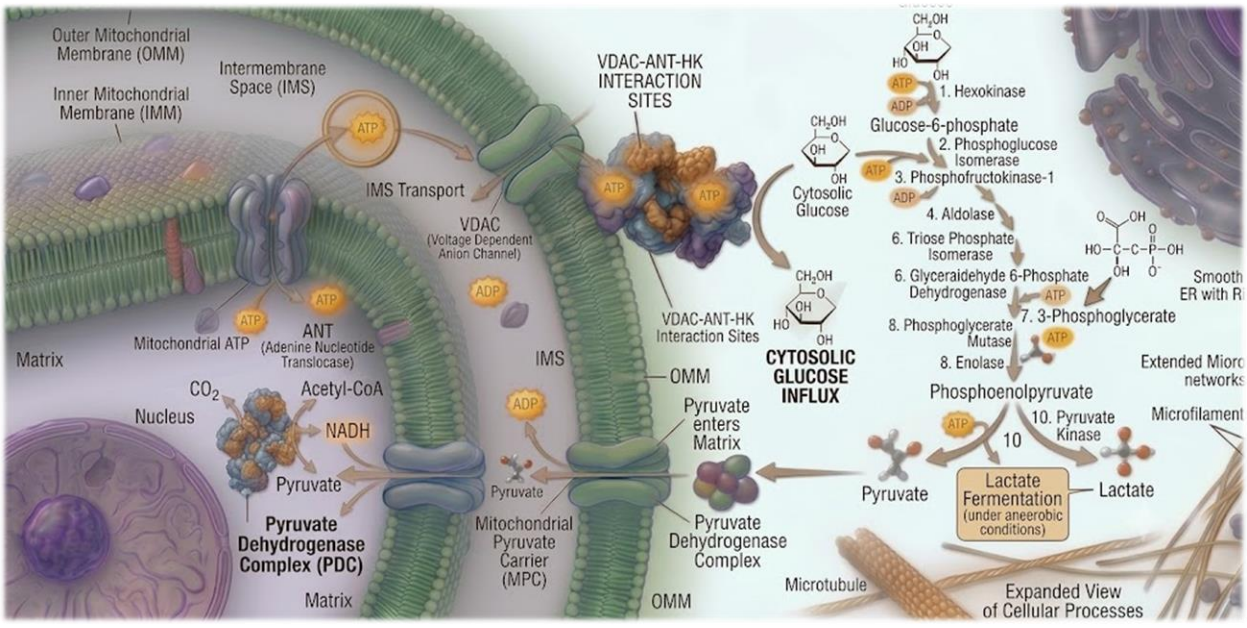

Figure 4: The Role of HKII in Coupling Mitochondrial ATP Production to Glucose Phosphorylation

I.5 The Strategic Use of G6P from Normal Human Cells

In healthy human cells, G6P produced via mitochondrial ATP is primarily directed toward glycogenesis or the glycolytic pathway to maintain steady-state energy levels. This localized synthesis ensures that cells can rapidly respond to fluctuations in glucose availability [37]. Furthermore, a portion of this G6P enters the pentose phosphate pathway to generate NADPH, which is essential for maintaining the cellular antioxidant defense system and lipid biosynthesis. Crucially, this pathway also produces ribose-5-phosphate, the sugar backbone for nucleotide synthesis; by balancing these metabolic outputs, the cell ensures it has the necessary precursors to support DNA replication and sustained **cell proliferation** [38].

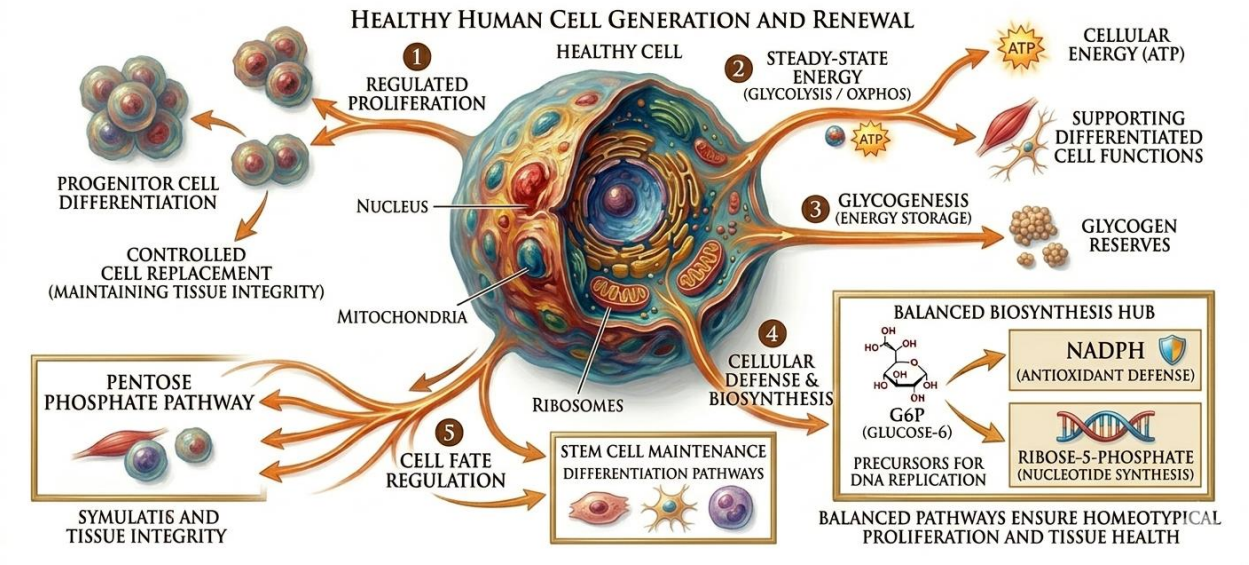

Figure 5: Regulated metabolism and renewal in healthy human cell (balanced proliferation, energy homeostasis and clear differentiation pathways)

I.6 The Multi-Purpose Use of G6P from Cancer Human Cells in Anabolism

In the context of oncology, cancer cells utilize G6P generated at the mitochondrial interface to fuel massive biosynthetic demands. This G6P serves as a precursor for the ribose-5-phosphate needed for nucleotide synthesis and for the production of amino acids [39]. By diverting mitochondrial-sourced G6P into anabolic pathways, cancer cells sustain **rapid proliferation** and biomass accumulation, effectively decoupling energy production from structural growth requirements [40].

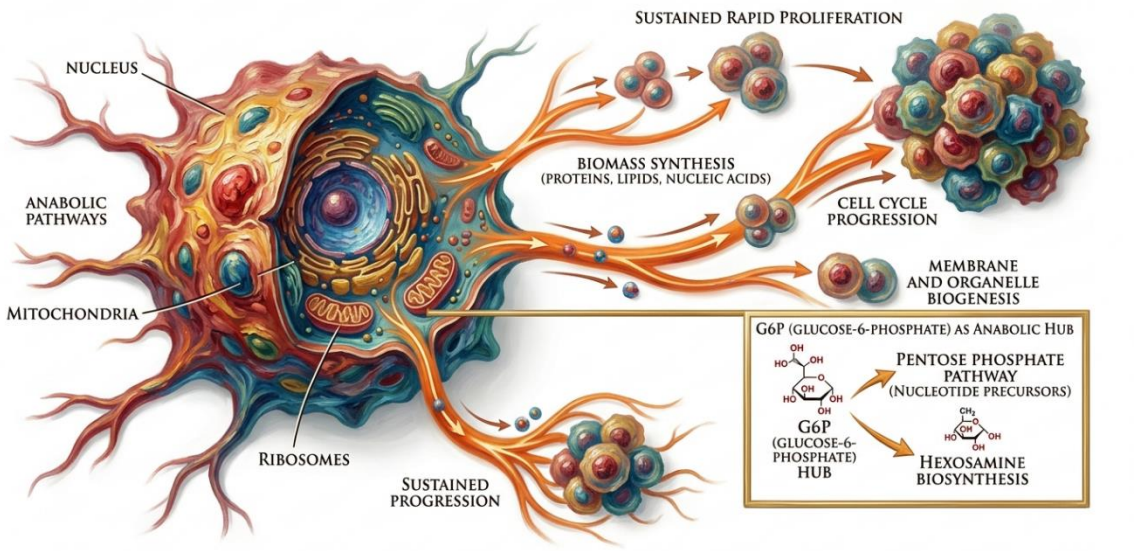

Figure 6: Metabolic reprogramming in proliferating cancer cells

I.7 Indirect functional effect of MitoNEET on Hexokinase II

MitoNEET indirectly modulates Hexokinase II (HKII) activity by regulating mitochondrial redox states and iron-sulfur cluster homeostasis [41]. Positive insights suggest that stabilized mitoNEET activity maintains the integrity of the outer mitochondrial membrane, facilitating efficient HKII-VDAC coupling for glucose phosphorylation [42]. Conversely, mitoNEET dysfunction can lead to excessive reactive oxygen species production, which negatively impacts HKII binding and impairs glycolytic flux in metabolic pathways [43].

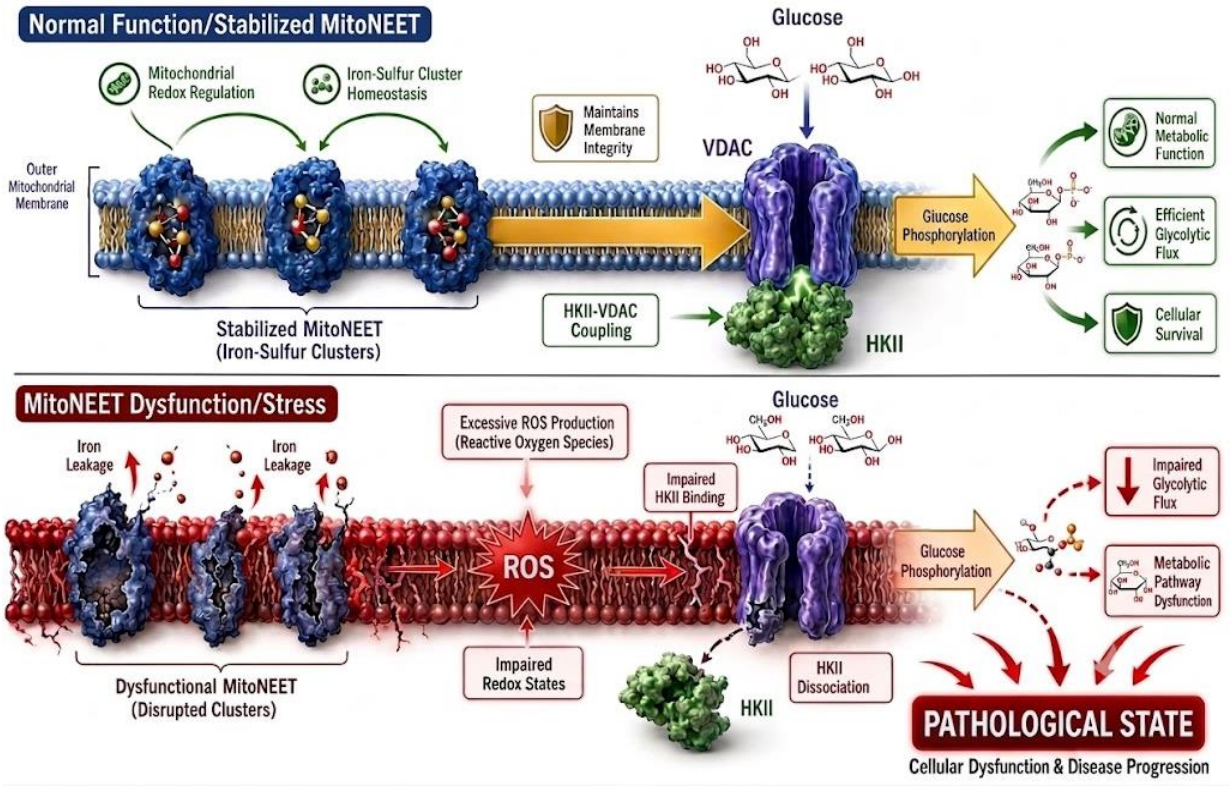

Figure 7: Schematic representation of the indirect functional effects of mitoNEET stability and dysfunction on Hexokinase II (HKII) binding and mitochondrial metabolic homeostasis.

I.8 The Mechanism of Healthy Cell Proliferation

Healthy cell division isn't just about signals; it's about **metabolic integration**. The cell ensures that energy production (Mitochondria) and building-block synthesis (Glucose Metabolism) are physically and chemically linked [44].

I.8.1 The Mitochondrial Foundation

Before a cell can divide, it must secure its energy supply and maintain redox balance.

- **MitoNEET: The Gatekeeper:** Located on the outer mitochondrial membrane, the protein **mitoNEET** serves as a regulatory hub. It manages iron-sulfur cluster transfers and electron transport, maintaining mitochondrial integrity so the "power plant" is ready for high-demand output [45].

- **High-Efficiency ATP Generation:** With mitoNEET ensuring stability, the mitochondria ramp up the **Electron Transport Chain (ETC)**. This produces the massive amounts of ATP (chemical energy) needed to fuel the synthesis of new cellular components [46].

I.8.2 Glucose Metabolism and Growth Coupling

To grow, the cell must "trap" and transform glucose. It does this by physically docking its metabolic machinery onto the mitochondria [47].

- **Strategic Localization of Hexokinase II (HKII):** The cell moves HKII to the mitochondrial surface. By being physically close, HKII can "grab" ATP the moment it exits the mitochondria, significantly increasing the enzyme's efficiency [48].
- **The Glucose-ATP Bridge:** This physical coupling ensures that the rate of glucose entry is directly proportional to the cell's energy output. It creates a seamless flow from raw fuel to processed energy [49].
- **G6P Generation:** Using that immediate supply of mitochondrial ATP, HKII phosphorylates glucose into **Glucose-6-Phosphate (G6P)**. This "traps" the sugar inside the cell, committing it to the proliferation cycle [50].

I.8.3 Driving the Proliferation Process

Once G6P is generated, it is diverted away from simple energy burning and toward "construction."

- **Fueling the Pentose Phosphate Pathway (PPP):** The cell funnels G6P into the PPP.
- **The Building Blocks:** This pathway produces:
    - **Nucleotides:** For DNA replication and RNA synthesis.
    - **NADPH:** For lipid synthesis and membrane building.

By integrating mitoNEET stability, ATP efficiency, and HKII localization, the cell creates a high-speed production line that converts glucose into a new daughter cell [51].

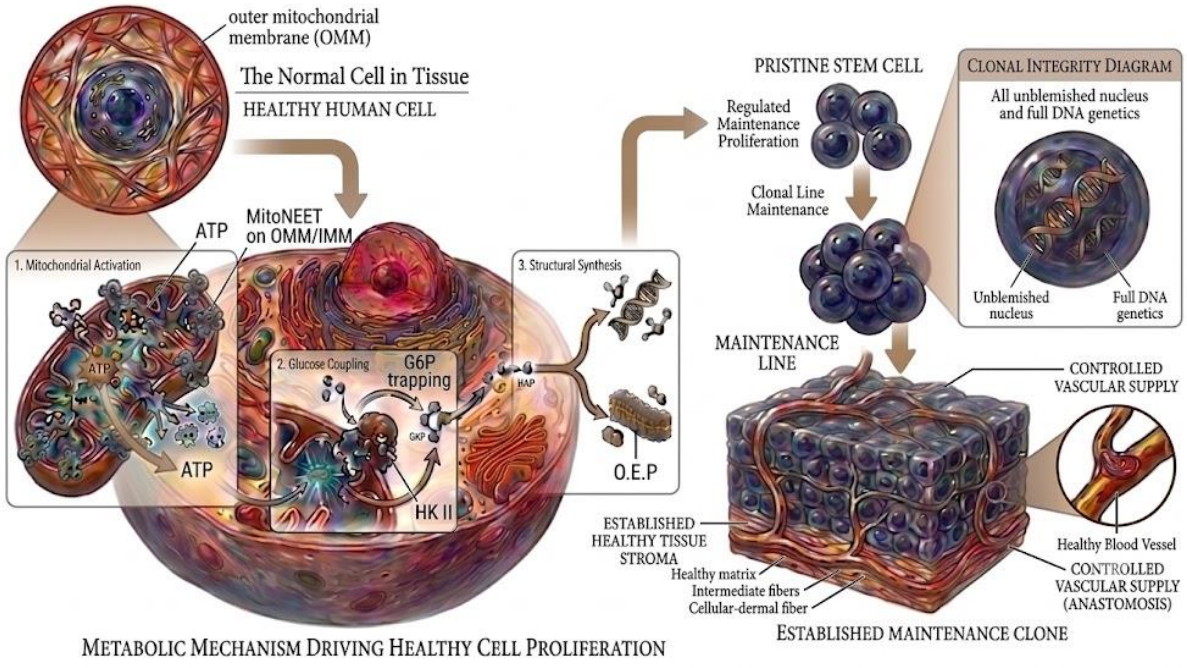

Figure 8: The Metabolic Biology of Healthy Cell Proliferation

I.9 Drug Repurposing in Cancer Research

I.9.1 Concept and Advantages of Drug Repurposing

Drug repurposing involves finding new medical uses for medications that are already approved by health authorities [52]. This approach reduces the risks related to drug safety and how the body processes the medicine, since their side effects are already well-understood [53]. In the field of cancer research, where developing a single new drug can cost over $2 billion, repurposing provides a faster and more affordable route to clinical testing [54]. Well-known examples of this strategy include using the diabetes drug metformin and the sedative thalidomide as cancer treatments [56].

I.9.2 Computational Approaches for Drug Repurposing

Developments in computer science and biology have made digital screening an essential first step in discovering new medicines [57]. Through a process called molecular docking, researchers can simulate how a drug molecule fits into a specific protein to predict how well they bind together [58]. This structure-based approach allows scientists to virtually test thousands of already

approved medications against targets like HKII, helping them identify the most promising candidates before beginning laboratory experiments [59].

I.9.3 Relevance to Pioglitazone

Pioglitazone is a strong candidate for repurposing because it is already proven to be safe and is known to affect how cells use energy [60]. Research indicates that drugs in this category, called thiazolidinediones, can reduce the activity of enzymes involved in sugar metabolism across different tissues [61]. Additionally, computer modeling suggests that the shape and chemical structure of pioglitazone allow it to fit into the active sites of the HKII enzyme, where it may compete with glucose or ATP to block the enzyme's function [62].

I.10 Bibliometric Trends in Repurposing

Provide a quantitative assessment of the research landscape, bibliometric data was extracted from the **Dimensions database** (available at URL: https://app.dimensions.ai/). This platform allows for a comprehensive analysis of global publication trends, helping to contextualize the significance of both the broad research field and the specific thesis objectives.

I.10.1 The Global Importance of the Research Field

As illustrated in **Figure 08**, the data retrieved from Dimensions using the keyword **"Drug Repurposing"** demonstrates an exponential increase in scientific output over the last 15 years. From a relatively modest volume of publications in 2010 (under 1,000), the field has surged to over 33,000 publications by 2025.

This trend highlights the critical importance of drug repositioning in modern medicine. The scientific community is increasingly prioritizing this strategy because it leverages existing safety profiles of known drugs, thereby accelerating the delivery of treatments to patients while minimizing the high costs and failure rates associated with traditional drug discovery.

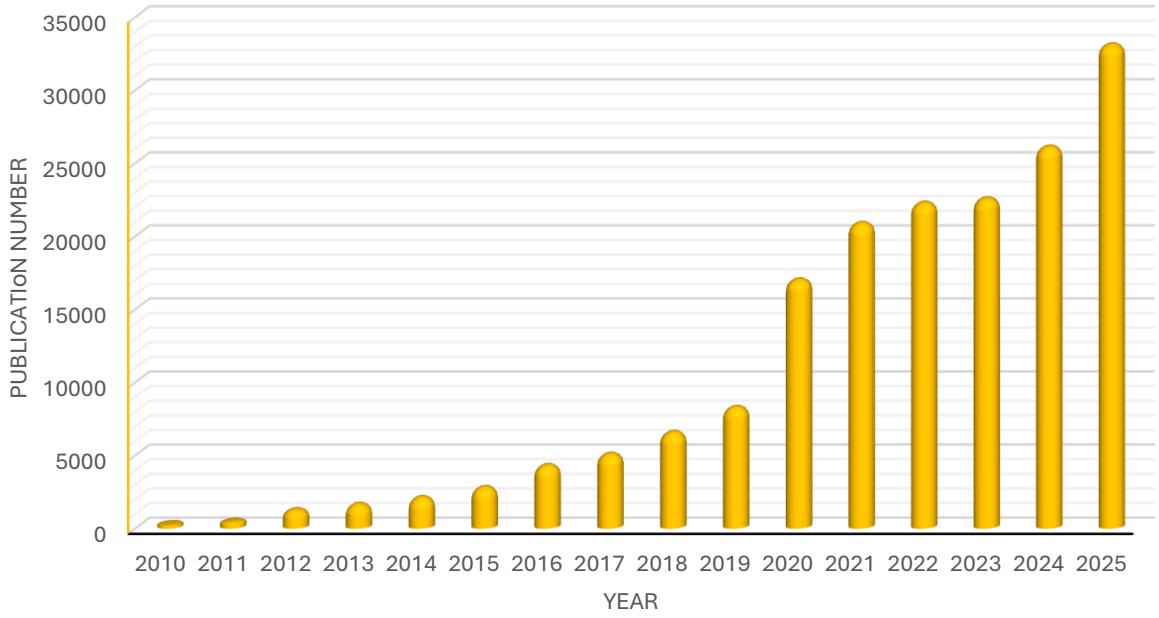

Figure 9: Global Publication Trends in the Field of Drug Repurposing (2010–2025)

I.10.2 The Strategic Importance of the Thesis Topic

Figure 10 presents the publication trends specifically related to the intersection of **In silico Drug Repurposing, Pioglitazone, Hexokinase II, Molecular Docking, and Cancer Metabolism** (These keywords were extracted from the thesis title and used together to obtain statistical data). The data from Dimensions reveals several key insights:

- **Timeliness:** After an initial period of early exploration between 2012 and 2016, there has been a notable and sustained increase in research activity.
- **Current Relevance:** The peak in publication numbers between 2023 and 2025 confirms that the targeting of cancer metabolism (specifically Hexokinase II) through computational modeling is currently a high-priority area in oncology.
- **Scientific Specialism:** While "Drug Repurposing" is a massive global field, this specific thesis topic operates within a specialized and rapidly growing niche. The recent spike in data points to a growing consensus on the potential of Pioglitazone as a candidate for metabolic-based cancer therapies.

By utilizing the **Dimensions** platform to track these metrics, it is evident that the thesis topic is not only scientifically sound but also highly relevant to the contemporary trajectory of pharmaceutical research and computational drug design.

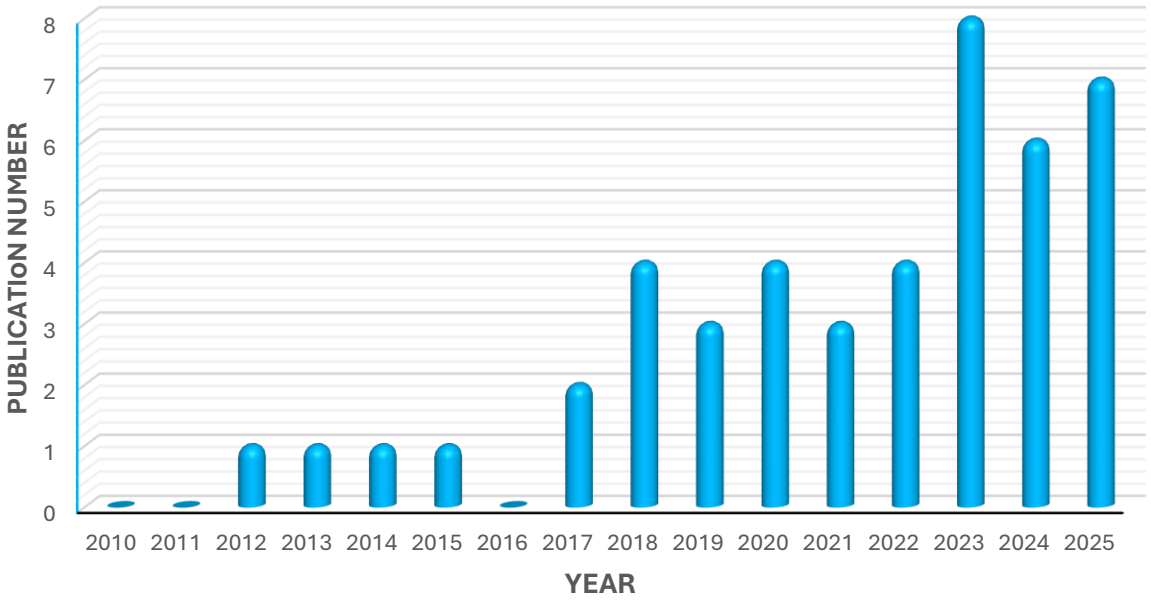

Figure 10: Evolution of Computational Research on Pioglitazone and Hexokinase II Interactions

I.11 Objectives and Scope of the Study

I.11.1 General objective and Research Gap

The primary aim of this research is to evaluate the potential of pioglitazone as a selective inhibitor of cancer-associated Hexokinase II through integrated *in silico* computational approaches, providing a molecular basis for its repurposing in cancer therapy. **Research Gap** to be addressed**:** Limited evidence exists regarding the interaction of pioglitazone with cancer-associated Hexokinase II and its potential as a repurposed anticancer agent. This gap can be addressed through an integrated in silico investigation combining molecular optimization, docking analysis, binding interaction visualization, ADME assessment, and toxicity prediction.

I.11.2 Specific objectives

- **Structural Acquisition:** To retrieve the high-resolution 3D crystal structure of human **MitoNEET** (PDB ID: **6DE9**) and prepare the protein for docking by removing water molecules and adding polar hydrogens.
- **Ligand optimization:** To generate the 3D structure of pioglitazone and perform geometry optimization using force-field methods to ensure the most energetically favorable conformation for docking.
- **Molecular Docking:** To execute site-directed molecular docking to predict the binding affinity ($kcal/mol$) and identify key amino acid residues involved in the pioglitazone MitoNEET interaction.
- **Comparative Analysis:** To compare the binding energy and interaction profile of pioglitazone with standard MitoNEET inhibitors, such as Furosemide to assess its relative potency

References

[1] Lu J, Tan M, Cai Q. The Warburg effect in tumor progression: mitochondrial oxidative metabolism as an anti-metastasis mechanism. Cancer Lett. 2015 Jan 28;356(2 Pt A):156-64. doi: 10.1016/j.canlet.2014.04.001. Epub 2014 Apr 13. PMID: 24732809; PMCID: PMC4195816.

[2] Pedersen PL. Warburg, me and Hexokinase 2: Multiple discoveries of key molecular events underlying one of cancers' most common phenotypes, the "Warburg Effect", i.e., elevated glycolysis in the presence of oxygen. J Bioenerg Biomembr. 2007 Jun;39(3):211-22. doi: 10.1007/s10863-007-9094-x. PMID: 17879147.

[3] Vyssokikh MY, Brdiczka D. The function of complexes between the outer mitochondrial membrane pore (VDAC) and the adenine nucleotide translocase in regulation of energy metabolism and apoptosis. Acta Biochim Pol. 2003;50(2):389-404. PMID: 12833165.

[4] Xia, Y., Sun, M., Huang, H. et al. Drug repurposing for cancer therapy. Sig Transduct Target Ther 9, 92 (2024). https://doi.org/10.1038/s41392-024-01808-1

[5] Shaik, S., Dey, T., Irene, P. R., Kant, K., Kurmi, S. P. C., DR, N., Gupta, R. K., Kurmi, S. K., M. S., A., & Thapa, S. (2025). Repurposing troglitazone and pioglitazone as breast cancer therapeutics: An integrated computational study. In Silico Research in Biomedicine, 1, 100108. https://doi.org/10.1016/j.insi.2025.100108

[6] Ninomiya, I., Yamazaki, K., oyama, K., Hayashi, H., Tajima, H., Kitagawa, H., Fushida, S., Fujimura, T., & ohta, T. (2014). Pioglitazone inhibits the proliferation and metastasis of human pancreatic cancer cells. *oncology letters*, *8*(6), 2709–2714. https://doi.org/10.3892/ol.2014.2553

[7] Wang, Y., Zhang, R., Chen, Q., Lei, Z., Shi, C., Pang, Y., Zhang, S., He, L., Xu, L., Xing, J., Guo, H. (2024). PPARγ Agonist Pioglitazone Prevents Hypoxia-induced Cardiac Dysfunction by Reprogramming Glucose Metabolism. International Journal of Biological Sciences, 20(11), 4297-4313. https://doi.org/10.7150/ijbs.98387.

[8] Kandasamy, T., Sarkar, S., & Ghosh, S. S. (2024). Harnessing Drug Repurposing to Combat Breast Cancer by Targeting Altered Metabolism and Epithelial-to-Mesenchymal Transition

Pathways. *ACS pharmacology & translational science*, *7*(12), 3780–3794. https://doi.org/10.1021/acsptsci.4c00545.

[9] Ciaramella, V., Sasso, F. C., Di Liello, R., Corte, C. M. D., Barra, G., Viscardi, G., Esposito, G., Sparano, F., Troiani, T., Martinelli, E., orditura, M., De Vita, F., Ciardiello, F., & Morgillo, F. (2019). Activity and molecular targets of pioglitazone via blockade of proliferation, invasiveness and bioenergetics in human NSCLC. Journal of experimental & clinical cancer research : CR, 38(1), 178. https://doi.org/10.1186/s13046-019-1176-1.

[10] Mosure, S. A., Shang, J., Eberhardt, J., Brust, R., Zheng, J., Griffin, P. R., Forli, S., & Kojetin, D. J. (2019). Structural Basis of Altered Potency and Efficacy Displayed by a Major in Vivo Metabolite of the Antidiabetic PPARγ Drug Pioglitazone. *Journal of medicinal chemistry*, *62*(4), 2008–2023. https://doi.org/10.1021/acs.jmedchem.8b01573

[11] Lee, M. A., Tan, L., Yang, H., Im, Y. G., & Im, Y. J. (2017). Structures of PPARγ complexed with lobeglitazone and pioglitazone reveal key determinants for the recognition of antidiabetic drugs. *Scientific reports*, *7*(1), 16837. https://doi.org/10.1038/s41598-017-17082-x

[12] Galli, A., Ceni, E., Crabb, D. W., Mello, T., Salzano, R., Grappone, C., Milani, S., Surrenti, E., Surrenti, C., & Casini, A. (2004). Antidiabetic thiazolidinediones inhibit invasiveness of pancreatic cancer cells via PPARgamma independent mechanisms. Gut, 53(11), 1688–1697. https://doi.org/10.1136/gut.2003.031997

[13] Triplitt, C., Cersosimo, E., & DeFronzo, R. A. (2010). Pioglitazone and alogliptin combination therapy in type 2 diabetes: a pathophysiologically sound treatment. Vascular health and risk management, 6, 671–690. https://doi.org/10.2147/vhrm.s4852

[14] Desouza, C. V., & Shivaswamy, V. (2010). Pioglitazone in the treatment of type 2 diabetes: safety and efficacy review. Clinical medicine insights. Endocrinology and diabetes, 3, 43–51. https://doi.org/10.4137/cmed.s5372

[15] Camponeschi, F., Piccioli, M., & Banci, L. (2022). The Intriguing mitoNEET: Functional and Spectroscopic Properties of a Unique [2Fe-2S] Cluster Coordination Geometry. Molecules (Basel, Switzerland), 27(23), 8218. https://doi.org/10.3390/molecules27238218

[16] ohama, Y., Harada, T., Iwabe, T., Taniguchi, F., Takenaka, Y., & Terakawa, N. (2008). Peroxisome proliferator-activated receptor-gamma ligand reduced tumor necrosis factor-alpha-induced interleukin-8 production and growth in endometriotic stromal cells. Fertility and sterility, 89(2), 311–317. https://doi.org/10.1016/j.fertnstert.2007.03.061

[17] Waugh, J., Keating, G. M., Plosker, G. L., Easthope, S., & Robinson, D. M. (2006). Pioglitazone: a review of its use in type 2 diabetes mellitus. Drugs, 66(1), 85–109. https://doi.org/10.2165/00003495-200666010-00005

[18] Devchand, P. R., Liu, T., Altman, R. B., FitzGerald, G. A., & Schadt, E. E. (2018). The Pioglitazone Trek via Human PPAR Gamma: From Discovery to a Medicine at the FDA and Beyond. Frontiers in pharmacology, 9, 1093. https://doi.org/10.3389/fphar.2018.01093

[19] Lin, J., Zhou, T., Ye, K., & Wang, J. (2007). Crystal structure of human mitoNEET reveals distinct groups of iron sulfur proteins. Proceedings of the National Academy of Sciences of the United States of America, 104(37), 14640–14645. https://doi.org/10.1073/pnas.0702426104

[20] Cui Y, Song Y, Yan S, Cao M, Huang J, Jia D, Liu Y, Zhang S, Fan W, Cai L, Li C, Xing Y. CUEDC1 inhibits epithelial-mesenchymal transition via the TβRI/Smad signaling pathway and suppresses tumor progression in non-small cell lung cancer. Aging (Albany NY). 2020 oct 25;12(20):20047-20068. doi: 10.18632/aging.103329. Epub 2020 oct 25. PMID: 33099540; PMCID: PMC7655170

[21] Pizcueta, P., Vergara, C., Emanuele, M., Vilalta, A., Rodríguez-Pascau, L., & Martinell, M. (2023). Development of PPARγ Agonists for the Treatment of Neuroinflammatory and Neurodegenerative Diseases: Leriglitazone as a Promising Candidate. International journal of molecular sciences, 24(4), 3201. https://doi.org/10.3390/ijms24043201

[22] Chakrabarty, R. P., & Chandel, N. S. (2022). Beyond ATP, new roles of mitochondria. The biochemist, 44(4), 2–8. https://doi.org/10.1042/bio_2022_119

[23] Stauch, K. L., Villeneuve, L. M., Totusek, S., Lamberty, B., Ciborowski, P., & Fox, H. S. (2019). Quantitative Proteomics of Presynaptic Mitochondria Reveal an overexpression and Biological Relevance of Neuronal MitoNEET in Postnatal Brain Development. Developmental neurobiology, 79(4), 370–386. https://doi.org/10.1002/dneu.22684

[24] Alberts B, Johnson A, Lewis J, et al. Molecular Biology of the Cell. 4th edition. New York: Garland Science; 2002. The Mitochondrion. Available from: https://www.ncbi.nlm.nih.gov/books/NBK26894/

[25] Wang, G., Lai, Y., Chen, X., Li, N., Zhong, C., Yan, Y., Ma, Q., Hong, X., Zhu, N., & Yu, W. (2025). Hexokinase 2 promotes tumor development and progression. American journal of cancer research, 15(10), 4499–4515. https://doi.org/10.62347/ZYNN3077

[26] Morelli, A. M., Ravera, S., & Panfoli, I. (2020). The aerobic mitochondrial ATP synthesis from a comprehensive point of view. *open biology*, *10*(10), 200224. https://doi.org/10.1098/rsob.200224

[27] Kusminski, C. M., Holland, W. L., Sun, K., Park, J., Spurgin, S. B., Lin, Y., Askew, G. R., Simcox, J. A., McClain, D. A., Li, C., & Scherer, P. E. (2012). MitoNEET-driven alterations in adipocyte mitochondrial activity reveal a crucial adaptive process that preserves insulin sensitivity in obesity. Nature medicine, 18(10), 1539–1549. https://doi.org/10.1038/nm.2899

[28] Liberti, M. V., & Locasale, J. W. (2016). The Warburg Effect: How Does it Benefit Cancer Cells?. Trends in biochemical sciences, 41(3), 211–218. https://doi.org/10.1016/j.tibs.2015.12.001

[29] Woldetsadik, A. D., Vogel, M. C., Rabeh, W. M., & Magzoub, M. (2017). Hexokinase II-derived cell-penetrating peptide targets mitochondria and triggers apoptosis in cancer cells. *FASEB journal : official publication of the Federation of American Societies for Experimental Biology*, *31*(5), 2168–2184. https://doi.org/10.1096/fj.201601173R

[30] Abbadi, S., Rodarte, J. J., Abutaleb, A., Lavell, E., Smith, C. L., Ruff, W., Schiller, J., olivi, A., Levchenko, A., Guerrero-Cazares, H., & Quinones-Hinojosa, A. (2014). Glucose-6-phosphatase is a key metabolic regulator of glioblastoma invasion. *Molecular cancer research : MCR*, *12*(11), 1547–1559. https://doi.org/10.1158/1541-7786.MCR-14-0106-T

[31] Maldonado, E. N., & Lemasters, J. J. (2012). Warburg revisited: regulation of mitochondrial metabolism by voltage-dependent anion channels in cancer cells. *The Journal of pharmacology and experimental therapeutics*, *342*(3), 637–641. https://doi.org/10.1124/jpet.112.192153

[32] Palsson-McDermott, E. M., & o'Neill, L. A. (2013). The Warburg effect then and now: from cancer to inflammatory diseases. *BioEssays : news and reviews in molecular, cellular and developmental biology*, *35*(11), 965–973. https://doi.org/10.1002/bies.201300084

[33] Nederlof, R., Eerbeek, o., Hollmann, M. W., Southworth, R., & Zuurbier, C. J. (2014). Targeting hexokinase II to mitochondria to modulate energy metabolism and reduce ischaemia-reperfusion injury in heart. British journal of pharmacology, 171(8), 2067–2079. https://doi.org/10.1111/bph.12363

[34] Ahamed, A., Hosea, R., Wu, S., & Kasim, V. (2023). The Emerging Roles of the Metabolic Regulator G6PD in Human Cancers. *International journal of molecular sciences*, *24*(24), 17238. https://doi.org/10.3390/ijms242417238

[35] Burns, J. S., & Manda, G. (2017). Metabolic Pathways of the Warburg Effect in Health and Disease: Perspectives of Choice, Chain or Chance. *International journal of molecular sciences*, *18*(12), 2755. https://doi.org/10.3390/ijms18122755

[36] Roberts, D., Miyamoto, S. Hexokinase II integrates energy metabolism and cellular protection: Akting on mitochondria and ToRCing to autophagy. Cell Death Differ 22, 248–257 (2015). https://doi.org/10.1038/cdd.2014.173

[37] Beneyton, T., Krafft, D., Bednarz, C., Kleineberg, C., Woelfer, C., Ivanov, I., Vidaković-Koch, T., Sundmacher, K., & Baret, J. C. (2018). out-of-equilibrium microcompartments for the bottom-up integration of metabolic functions. *Nature communications*, *9*(1), 2391. https://doi.org/10.1038/s41467-018-04825-1

[38] Song, J., Sun, H., Zhang, S., & Shan, C. (2022). The Multiple Roles of Glucose-6-Phosphate Dehydrogenase in Tumorigenesis and Cancer Chemoresistance. Life (Basel, Switzerland), 12(2), 271. https://doi.org/10.3390/life12020271

[39] Zhang, W., Jiao, H., Xue, J., Zhou, J., Wang, Y., Pan, Q., Guo, Y., Zhang, G., Hu, H., & Guo, X. (2026). Structures of the human glucose-6-phosphate transporter provide insights into its transport cycle and substrate recognition. *PLoS biology*, *24*(3), e3003731. https://doi.org/10.1371/journal.pbio.3003731

[40] Rajas, F., Gautier-Stein, A., & Mithieux, G. (2019). Glucose-6 Phosphate, A Central Hub for Liver Carbohydrate Metabolism. *Metabolites*, *9*(12), 282. https://doi.org/10.3390/metabo9120282

[41] Barahona, M. J., Salazar, K., & Nualart, F. (2025). The unanticipated role of the glial-associated glucose-6-phosphatase system in brain homeostasis. *iScience*, *28*(12), 114235. https://doi.org/10.1016/j.isci.2025.114235

[42] Karlstaedt, A., Khanna, R., Thangam, M., & Taegtmeyer, H. (2020). Glucose 6-Phosphate Accumulates via Phosphoglucose Isomerase Inhibition in Heart Muscle. *Circulation research*, *126*(1), 60–74. https://doi.org/10.1161/CIRCRESAHA.119.315180

[43] Kundu, B. K., Zhong, M., Sen, S., Davogustto, G., Keller, S. R., & Taegtmeyer, H. (2015). Remodeling of glucose metabolism precedes pressure overload-induced left ventricular hypertrophy: review of a hypothesis. Cardiology, 130(4), 211–220. https://doi.org/10.1159/000369782

[44] Mason, E. F., & Rathmell, J. C. (2011). Cell metabolism: an essential link between cell growth and apoptosis. *Biochimica et biophysica acta*, *1813*(4), 645–654. https://doi.org/10.1016/j.bbamcr.2010.08.011

[45] Chandel N. S. (2021). Metabolism of Proliferating Cells. Cold Spring Harbor perspectives in biology, 13(10), a040618. https://doi.org/10.1101/cshperspect.a040618

[46] Salazar-Roa, M., & Malumbres, M. (2017). Fueling the Cell Division Cycle. Trends in cell biology, 27(1), 69–81. https://doi.org/10.1016/j.tcb.2016.08.009

[47] Ward, P. S., & Thompson, C. B. (2012). Signaling in control of cell growth and metabolism. Cold Spring Harbor perspectives in biology, 4(7), a006783. https://doi.org/10.1101/cshperspect.a006783

[48] Tippetts, T. S., Sieber, M. H., & Solmonson, A. (2023). Beyond energy and growth: the role of metabolism in developmental signaling, cell behavior and diapause. Development (Cambridge, England), 150(20), dev201610. https://doi.org/10.1242/dev.201610

[49] Zhu, J., & Thompson, C. B. (2019). Metabolic regulation of cell growth and proliferation. Nature reviews. Molecular cell biology, 20(7), 436–450. https://doi.org/10.1038/s41580-019-0123-5

[50] Kalucka, J., Missiaen, R., Georgiadou, M., Schoors, S., Lange, C., De Bock, K., Dewerchin, M., & Carmeliet, P. (2015). Metabolic control of the cell cycle. Cell cycle (Georgetown, Tex.), 14(21), 3379–3388. https://doi.org/10.1080/15384101.2015.1090068

[51] Jáuregui-Wade, J. M., Valdés, J., Ayala-Sumuano, J. T., Ávila-García, R., & Cerbón-Solorzano, J. (2019). De novo synthesis of sphingolipids plays an important role during in vitro encystment of Entamoeba invadens. Biochemical and biophysical research communications, 508(4), 1031–1037. https://doi.org/10.1016/j.bbrc.2018.12.005

[52] Al Khzem, A. H., Gomaa, M. S., Alturki, M. S., Tawfeeq, N., Sarafroz, M., Alonaizi, S. M., Al Faran, A., Alrumaihi, L. A., Alansari, F. A., & Alghamdi, A. A. (2024). Drug Repurposing for Cancer Treatment: A Comprehensive Review. *International journal of molecular sciences*, *25*(22), 12441. https://doi.org/10.3390/ijms252212441

[53] Haddad, N., Gamaethige, S. M., Wehida, N., & Elbediwy, A. (2024). Drug Repurposing: Exploring Potential Anti-Cancer Strategies by Targeting Cancer Signalling Pathways. Biology, 13(6), 386. https://doi.org/10.3390/biology13060386

[54] Shahab, M., Al-Madhagi, H., Zheng, G. *et al.* Structure based virtual screening and molecular simulation study of FDA-approved drugs to inhibit human HDAC6 and VISTA as dual cancer immunotherapy. *Sci Rep* **13**, 14466 (2023). https://doi.org/10.1038/s41598-023-41325-9

[55] Latambale, G., & Juvale, K. (2025). Thiazolidinedione derivatives: emerging role in cancer therapy. Molecular diversity, 29(6), 5185–5217. https://doi.org/10.1007/s11030-024-11093-3

[56] Ranjan, G., Ranjan, S., Sunita, P., & Pattanayak, S. P. (2025). Thiazolidinedione derivatives in cancer therapy: exploring novel mechanisms, therapeutic potentials, and future horizons in oncology. Naunyn-Schmiedeberg's archives of pharmacology, 398(5), 4705–4725. https://doi.org/10.1007/s00210-024-03661-z

[57] Patra, K. C., & Hay, N. (2013). Hexokinase 2 as oncotarget. oncotarget, 4(11), 1862–1863. https://doi.org/10.18632/oncotarget.1563

[58] Ndidi, U. S., ogra, I. o., Jonathan, E. U., & Iroha, o. K. (2025). Drug repurposing in cancer research: a bibliometric analysis. *Discover oncology*, *16*(1), 1796. https://doi.org/10.1007/s12672-025-02895-4

[59] Muneer I, Ahmad S, Naz A, Abbasi SW, Alblihy A, Aloliqi AA, Aba Alkhayl FF, Alrumaihi F, Ahmad S, El Bakri Y, Tahir Ul Qamar M. Discovery of Novel Inhibitors From Medicinal Plants for V-Domain Ig Suppressor of T-Cell Activation. Front Mol Biosci. 2021 oct 26;8:716735. doi: 10.3389/fmolb.2021.716735. PMID: 34765641; PMCID: PMC8576517.

[60] Khan, S. A., Raza, K., Tiwari, P., El-Tanani, M., Rabbani, S. A., & Parvez, S. (2026). Mechanisms to medicines: navigating drug repurposing strategies in Alzheimer's disease. *Frontiers in aging neuroscience*, *17*, 1676065. https://doi.org/10.3389/fnagi.2025.1676065

[61] Wahab, S., Alsayari, A., Majrashi, T. A., Almoyad, M. A. A., Assiri, R. A., Ahmad, W., & Chandra, S. (2025). Exploring drug repurposing for PAK2 inhibition: a systematic virtual screening of FDA-approved drugs against cancer. *Discover oncology*, *16*(1), 1747. https://doi.org/10.1007/s12672-025-03516-w

[62] Xu, J., Li, X., & Jia, Y. (2025). Target screening and optimization of candidate compounds for breast cancer treatment using bioinformatics and computational chemistry approaches. *Frontiers in pharmacology*, *16*, 1467504. https://doi.org/10.3389/fphar.2025.1467504

Chapter II

Molecular Modeling Framework

II.1 Biomolecular Target Acquisition and Refinement

In structural biology and drug design, acquiring and refining a biomolecular target is the foundational step. It involves selecting a high-resolution protein structure from repositories like the PDB. Researchers then perform "refinement" by adding missing residues, optimizing hydrogen bonding networks, and ensuring the protein's geometry is energetically stable for simulations [63].

II.2 Structural Insights into the mitoNEET-Furosemide Complex

Metabolic reprogramming is a hallmark of oncogenesis, typically characterized by the shift toward aerobic glycolysis [64]. To investigate the potential of repurposing existing drugs to modulate this metabolic switch, researchers have pivoted from generalized models to specific ligand-bound structures, such as the human mitoNEET protein complexed with furosemide (PDB ID: **6DE9**) [65].

➢ Core Structural Features

The **6DE9** structure is critical for understanding direct pharmacological inhibition. MitoNEET is a **homodimeric protein** tethered to the outer mitochondrial membrane (oMM). Its architecture is defined by:

- **The [2Fe-2S] Clusters:** Each monomer houses an iron-sulfur cluster coordinated by an unconventional **3-Cys-1-His** motif. This rare His ligand renders the cluster sensitive to pH and redox changes, making it a "rheostat" for cellular metabolism [66].
- **The Dimeric Interface:** The protein functions as a single unit where the stability of these clusters dictates biochemical signaling pathways, particularly those governing **ferroptosis** and oxidative stress.

II.3 Furosemide Binding and Mechanism

The 6DE9 structure specifically illustrates how **furosemide**, a potent loop diuretic, interacts with the mitoNEET cytosolic domain. Unlike general docking simulations, this crystal structure reveals:

1. **Binding Site Affinity:** Furosemide binds in a pocket adjacent to the **[2Fe-2S] cluster**, stabilizing the protein in a way that prevents the premature release of the cluster.
2. **Inhibition of Cluster Transfer:** By occupying this site, furosemide modulates the protein's ability to transfer its iron-sulfur cargo to acceptor proteins, thereby disrupting the metabolic signals that fuel **cancer cell proliferation**.
3. **Redox Modulation:** The presence of the drug alters the electronic environment of the **3-Cys-1-His** coordination sphere, directly influencing the protein's midpoint potential (E_m) [67].

Key takeaway: Utilizing the 6DE9 model allows for high-resolution mapping of the furosemide-binding pocket. This is essential for future structure-based drug design (SBDD) aimed at enhancing the potency of mitoNEET ligands to combat metabolic dysregulation in cancer.

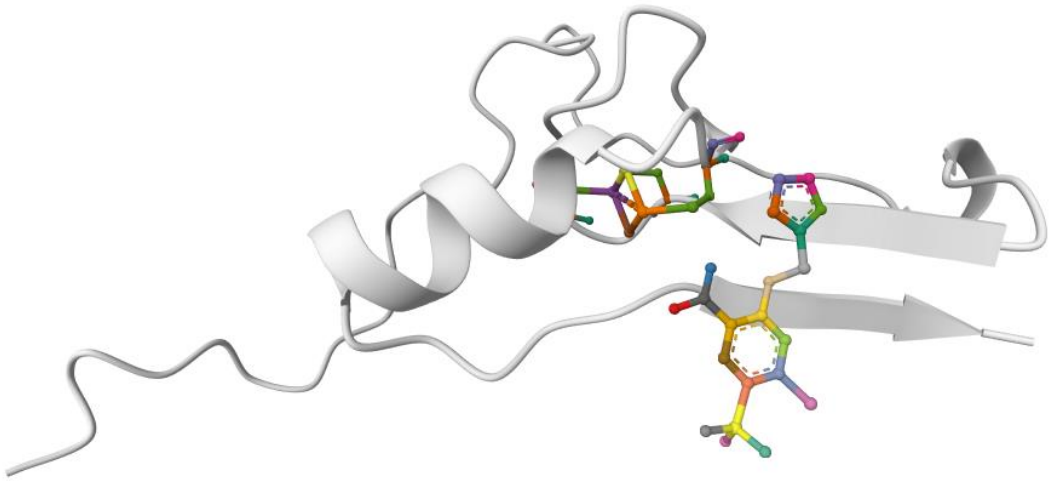

Figure 11: Crystal Structure of the Human mitoNEET Homodimer in Complex with Furosemide (PDB ID: 6DE9), highlighting the proximity of the ligand to the redox-active [2Fe-2S] centers.

II.4 Protein Preparation

The following steps outline the protein preparation stage:

1) Structure Retrieval and Quality Assessment

The process begins by obtaining the high-resolution experimental coordinates from the **RCSB Protein Data Bank (PDB)**.

- **Accessing the Entry:** The structure is retrieved using the unique identifier **6DE9**.
- **Data Verification:** The PDB header is reviewed to confirm experimental parameters. The structure boasts a resolution of **1.95 Å**, which is well below the 2.5 Å threshold typically required for reliable structure-based drug design (SBDD). This ensures that the positions of critical binding site residues and the **[2Fe-2S] cluster** are accurately defined [68].

2) Selection of the Biological Unit

MitoNEET is a **homodimer**, and the **6DE9** entry contains two identical protein chains (Chains A and B).

- **Monomer Isolation:** For the purpose of docking simulations, **Chain A** is typically isolated. Reducing the system to a monomer increases computational efficiency while maintaining the integrity of the active site, as the chains are functionally equivalent.
- **Alternate Conformation Cleanup:** In instances where residues possess multiple reported positions (alt-loc tags), the 'B' positions are pruned, retaining only the **primary high-occupancy atoms** to ensure a single, stable conformation [69-70].

3) Systematic Removal of Heteroatoms and Solvents

To prepare the pocket for ligand interaction studies, crystallographic "noise" must be eliminated.

- **Dehydration:** All crystallographic water molecules (HoH) are removed. This "empties" the pocket, allowing for the unbiased sampling of candidate molecules without interference from solvent molecules that may not be conserved during ligand binding [71].
- **De-liganding:** The native ligand (furosemide) is extracted from the binding site to create the "apo" receptor model.
- **Preservation of the [2Fe-2S] Cluster:** Crucially, the **FES cluster** (FES A 202) is retained. It remains coordinated to the redox-active site residues: **Cys72, Cys74, Cys83, and His87**.

- **Ion Stripping:** Non-essential ions from the purification buffer (e.g., chloride or sodium ions) are stripped to prevent artificial electrostatic interference during the scoring and docking phases [72].

4) Structural Repair and Hydrogenation

X-ray diffraction at 1.95 Å generally does not resolve light atoms (hydrogens) or highly flexible loops, necessitating chemical "completion" of the **6DE9** model.

- **Hydrogen Addition:** Missing hydrogen atoms are added to satisfy valency. This is essential for accounting for the hydrogen-bonding networks around the **[2Fe-2S] cluster**, particularly involving the His87-Lys55 interaction [73].
- **Protonation State Assignment:** The protonation states of ionizable residues (especially Histidine) are adjusted to a physiological **pH of 7.4** using tools like PROPKA to ensure realistic electrostatic interactions.
- **Modeling Missing Loops:** Any gaps in the sequence particularly in flexible regions of the cytosolic domain are reconstructed using homology modeling or loop refinement algorithms to ensure a continuous and stable protein surface [74].

5) Conversion to PDBQT Format

The transition from a standard .pdb file to a. pdbqt file is a critical step that integrates chemical properties into the structural coordinates. This format differs from the standard PDB by including **P**artial charges (q), **B**ond types, and **Q**uantified **T**orsions [75].

This rigorous preparation protocol ensures that the resulting model is a high-fidelity template, ready for accurate docking of novel inhibitors or repurposing studies.

II.4 Ligand Optimization

1) Preparation of Pioglitazone

The following steps detail the quantum mechanical protocols utilized to refine the molecular geometry of pioglitazone for high-precision docking:

2) Geometry optimization via Gaussian

The initial 2D representation of the ligand must be converted into a 3D conformer and refined using computational chemistry.

- **Input Preparation:** A starting 3D structure is generated (e.g., from a SMILES string) and used to create a Gaussian input file (.gjf).
- **Level of Theory:** A high-level optimization is performed, typically using the **B3LYP** functional and a **6-311G(d)** basis set. This ensures that the bond lengths, angles, and dihedrals reach their true energy minimum [76].
- **Frequency Analysis:** Following optimization, a frequency calculation is conducted to confirm the absence of imaginary frequencies, ensuring the structure represents a true stationary point on the potential energy surface.

3) Electronic Property Calculation

Accurate docking depends heavily on the electrostatic complementarity between the ligand and the **6DE9** binding pocket.

- **Electrostatic Potential (ESP):** During the Gaussian run, the molecular electrostatic potential is mapped. This is critical for predicting how the ligand will align with polar residues in the hexokinase active site [77].
- **Population Analysis:** Using the optimized density, partial atomic charges are derived. While Gaussian provides various schemes, these results are essential for the subsequent transition to the docking force field [78].

4) Definition of Rotatable Bonds

To allow the docking algorithm to explore the ligand's flexibility, the molecule's degrees of freedom must be defined.

- **Torsion Tree Construction:** Tools like **AutoDockTools (MGLTools)** are used to identify "active" rotatable bonds.

- **Constraint Assignment:** Non-rotatable bonds, such as those within aromatic rings or double bonds, are "frozen" to maintain their structural integrity during the simulation [79].

5) Conversion to PDBQT Format

The final step integrates the geometric and electronic data into the specific file format required by the docking engine.

- **Charge Assignment:** The charges derived from Gaussian or standard schemes (such as **Gasteiger**) are mapped onto the atoms.
- **Atom Typing:** Each atom is assigned an AutoDock-compatible type (e.g., 'C' for aliphatic carbon, 'A' for aromatic carbon) to define its Van der Waals parameters.
- **Final output:** The resulting .pdbqt file contains the atomic coordinates, the partial charges (q), and the torsional tree information, completing the ligand's readiness for interaction with the **6DE9** receptor [80].

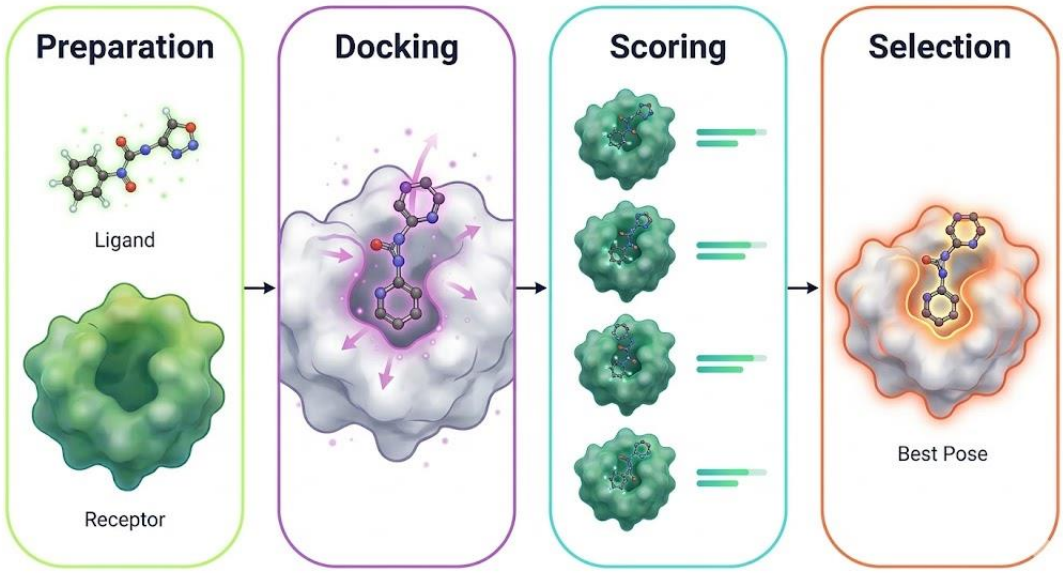

Figure 12: Workflow of the Molecular Docking Process

II.5 Reference Compounds

To establish a quantitative baseline for evaluating the binding affinity and inhibitory efficacy of Pioglitazone, **Furosemide** was utilized as the primary reference standard under identical computational parameters [81]. Although traditionally known as a loop diuretic, Furosemide has been identified as a potent modulator of **mitoNEET (CISD1)**, providing a high-resolution structural benchmark through its co-crystallized complex (PDB ID: **6DE9**) [82].

By targeting the unique **[2Fe-2S] cluster** environment, Furosemide serves as a critical structural and functional comparative model to validate the docking protocol. Unlike generalized TZD ligands, the availability of the **6DE9** crystal structure allows for a direct comparison between the predicted binding poses of Pioglitazone and the experimentally determined coordinates of Furosemide. This established binding profile provides a reliable metric for interpreting the thermodynamic parameters, such as the binding free energy (Delta G) [83].

Key Comparison Metrics

The use of Furosemide as a benchmark is justified by several factors:

- **Structural Validation:** It occupies a well-defined pocket adjacent to the iron-sulfur cluster, stabilizing the cytosolic domain.
- **Mechanism of Action:** Like the thiazolidinediones, it influences the redox potential and cluster stability, which are central to its role in regulating **ferroptosis** and metabolic flux.
- **Computational Accuracy:** Utilizing the 6DE9 structure as a reference reduces the reliance on homology modeling, ensuring that the docking grid and scoring functions are calibrated against a native ligand-bound state [84-85].

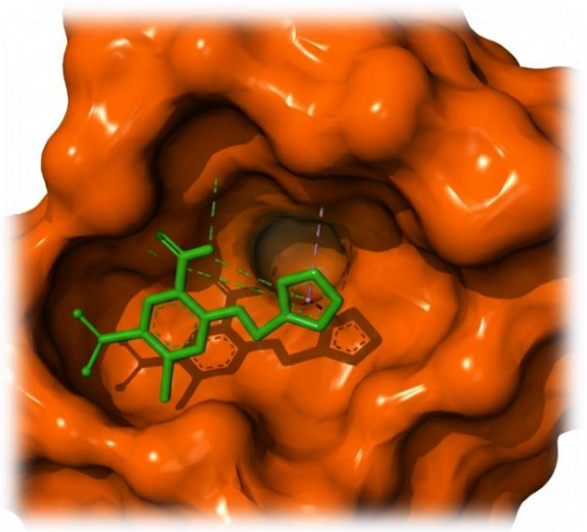

Figure 13: Native Binding Mode of the Reference Inhibitor Furosemide within the Human mitoNEET Cytosolic Pocket (PDB ID: 6DE9).

II.6 In Silico Drug Discovery Profiling

II.6.1 Molecular Docking Strategy

II.6.1.1 Grid Box Generation and Active Site Identification

Following the preparatory phases, molecular docking was deployed to predict the preferred orientation of ligands within the human mitoNEET receptor, specifically utilizing the **6DE9** crystal structure. Unlike the apo-state models, **6DE9** provides a high-resolution template of the protein already complexed with **furosemide**, offering a direct pharmacological roadmap of the binding pocket [86]. The molecular grid box is strategically centered, with the coordinates defined by the co-crystallized furosemide ligand in the 6DE9 model. This approach ensures that the search space is focused on the redox-active microenvironment [87].

By constraining the grid to this functional pocket, the simulation avoids computational overhead and minimizes the risk of identifying false-positive binding modes in non-functional peripheral regions of the protein surface [88].

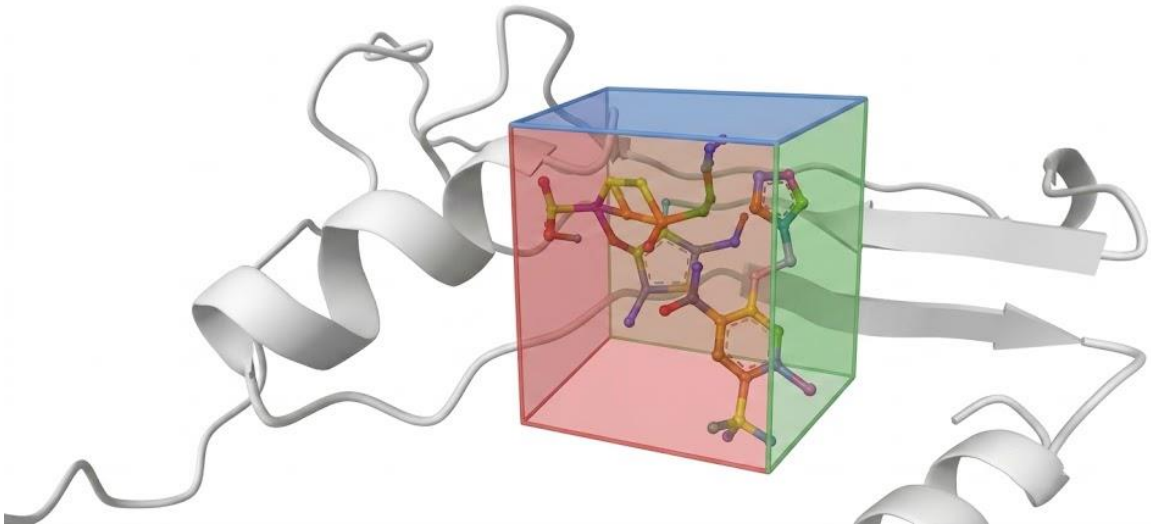

Figure 14: Grid Box Definition for the Ligand Binding Site of Human mitoNEET.

The docking grid box was centered on the furosemide-binding cavity of the crystallographic structure (PDB ID: **6DE9**) to enable accurate and targeted docking simulations within the cluster-binding domain.

II.6.1.2 Docking Parameters and Scoring Functions

The docking simulations were executed using the Iterated Local Search global optimizer algorithm integrated within AutoDock Vina [89]. To maximize the conformational sampling of the flexible pioglitazone molecule, the algorithm's exhaustiveness parameter was set to an elevated level. This ensures a rigorous search for the global energy minimum among the generated binding poses, reducing the likelihood of the algorithm becoming trapped in local energetic minima [90].

AutoDock Vina utilizes an empirical scoring function to estimate the theoretical binding affinity, denoted as ΔG°, expressed in kcal/mol. The scoring function evaluates steric interactions, hydrogen bonding, and hydrophobic interactions [91]. once the ΔG° for the highest-ranked pose was determined, the theoretical inhibition constant (K_i) was derived using the standard thermodynamic equation:

$$K_i = \exp\left(-\frac{\Delta G^\circ}{RT}\right), \quad \text{Equation II- 1}$$

With

$$\Delta G^\circ = -RT \ln K_i, \quad \text{Equation II- 2}$$

where R is the ideal gas constant (1.987×10^{-3} kcal/(K·mol)) and T represents the standard physiological temperature (298.15 K). This conversion translates the energetic metric into a clinically relevant biochemical parameter [92].

II.6.1.3 Validation of the Docking Protocol

To verify the reproducibility and spatial accuracy of the defined docking protocol, a redocking validation procedure was undertaken. The native co-crystallized ligand was computationally extracted from the 6DE9 structure and subsequently re-docked into the defined grid box covering the target pocket within the protein structure [93]. The geometric deviation between the experimentally determined crystallographic pose and the computationally predicted highest-ranked pose was measured. The protocol is considered mathematically valid and highly reliable when the Root Mean Square Deviation (RMSD) falls strictly below the acceptable threshold of 2.0 [94].

II.6.2 ADME-Tox and Pharmacoinformatics Profiling

Following the establishment of theoretical binding efficacy, the compound was subjected to comprehensive pharmacoinformatics profiling to evaluate its translational potential. In silico Absorption, Distribution, Metabolism, and Excretion (ADME) properties were predicted utilizing the **SwissADME** web architecture [95]. The primary filter applied was Lipinski's Rule of Five (Ro5), which assesses drug-likeness based on molecular weight, lipophilicity (LogP), and the number of hydrogen bond donors and acceptors [96].

Further pharmacokinetic evaluation centered on critical distribution metrics, primarily Gastrointestinal (GI) absorption and Blood-Brain Barrier (BBB) permeability. These parameters were visualized and predicted using the BoILED-Egg (Brain or IntestinaL EstimateD permeation method) predictive model. The BoILED-Egg plot maps the physicochemical space defined by

lipophilicity and topological polar surface area (TPSA), allowing for a rapid, robust classification of the molecule's passive absorption characteristics [97].

II.6.3 Toxicity Assessment

To rigorously evaluate the safety profile of repurposing pioglitazone for oncological therapeutics, researchers deployed advanced computational modeling platforms to predict potential adverse effects. Utilizing the ProTox-II automated web server, the study simulated both acute and chronic toxicity parameters *in silico* [98]. A primary metric established was the theoretical median lethal dose (LD_{50}), which enabled the quantitative categorization of the drug's safety window according to Globally Harmonized System (GHS) international standards.

Beyond systemic lethality, the toxicological screening focused on organ-specific vulnerabilities and cellular integrity. Given that thiazolidinediones undergo extensive hepatic metabolism, the computational workflow specifically scrutinized potential hepatotoxicity profiles to predict risk levels for drug-induced liver injury (DILI) [99]. Furthermore, the platform evaluated critical endpoints including mutagenicity, carcinogenicity, and immunotoxicity to ensure the molecule does not induce genomic instability or adverse immune responses. By mapping these pharmacoinformatics endpoints, the study establishes a baseline safety framework, suggesting that the therapeutic concentrations required for target inhibition fall well within a predictable and manageable safety margin for clinical translation.

References

[63] Fontenot, C. R., Cheng, Z., & Ding, H. (2022). Nitric oxide reversibly binds the reduced [2Fe-2S] cluster in mitochondrial outer membrane protein mitoNEET and inhibits its electron transfer activity. Frontiers in molecular biosciences, 9, 995421. https://doi.org/10.3389/fmolb.2022.995421

[64] Batool, M., Ahmad, B., & Choi, S. (2019). A Structure-Based Drug Discovery Paradigm. International journal of molecular sciences, 20(11), 2783. https://doi.org/10.3390/ijms20112783

[65] Geldenhuys, W. J., Long, T. E., Saralkar, P., Iwasaki, T., Nuñez, R. A. A., Nair, R. R., Konkle, M. E., Menze, M. A., Pinti, M. V., Hollander, J. M., Hazlehurst, L. A., & Robart, A. R. (2019). Crystal structure of the mitochondrial protein mitoNEET bound to a benze-sulfonide ligand. Communications chemistry, 2, 77. https://doi.org/10.1038/s42004-019-0172-x

[66] Landry, A. P., Wang, Y., Cheng, Z., Crochet, R. B., Lee, Y. H., & Ding, H. (2017). Flavin nucleotides act as electron shuttles mediating reduction of the [2Fe-2S] clusters in mitochondrial outer membrane protein mitoNEET. *Free radical biology & medicine*, *102*, 240–247. https://doi.org/10.1016/j.freeradbiomed.2016.12.001

[67] Landry, A. P., & Ding, H. (2014). Redox control of human mitochondrial outer membrane protein MitoNEET [2Fe-2S] clusters by biological thiols and hydrogen peroxide. The Journal of biological chemistry, 289(7), 4307–4315. https://doi.org/10.1074/jbc.M113.542050

[68] Tasnim, H., & Ding, H. (2022). Electron transfer activity of the nanodisc-bound mitochondrial outer membrane protein mitoNEET. Free radical biology & medicine, 187, 50–58. https://doi.org/10.1016/j.freeradbiomed.2022.05.011

[69] Ponto, L. L., & Schoenwald, R. D. (1990). Furosemide (frusemide). A pharmacokinetic/pharmacodynamic review (Part I). Clinical pharmacokinetics, 18(5), 381–408. https://doi.org/10.2165/00003088-199018050-00004

[70] Skolik, R. A., Geldenhuys, W. J., Konkle, M. E., & Menze, M. A. (2023). Biochemical Control of the Mitochondrial Protein MitoNEET by Biological Thiols and Lipid-derived Electrophiles. Advances in redox research, 7, 100059. https://doi.org/10.1016/j.arres.2022.100059

[71] Hou, X., Liu, R., Ross, S., Smart, E. J., Zhu, H., & Gong, W. (2007). Crystallographic studies of human MitoNEET. The Journal of biological chemistry, 282(46), 33242–33246. https://doi.org/10.1074/jbc.C700172200

[72] Bassani, D., Pavan, M., Sturlese, M., & Moro, S. (2022). Sodium or Not Sodium: Should Its Presence Affect the Accuracy of Pose Prediction in Docking GPCR Antagonists?. Pharmaceuticals (Basel, Switzerland), 15(3), 346. https://doi.org/10.3390/ph15030346

[73] Thomas, A., Benhabiles, N., Meurisse, R., Ngwabije, R., & Brasseur, R. (2001). Pex, analytical tools for PDB files. II. H-Pex: noncanonical H-bonds in alpha-helices. Proteins, 43(1), 37–44. https://doi.org/10.1002/1097-0134(20010401)43:1<37::aid-prot1015>3.0.co;2-l

[74] Wieduwilt, E. K., Macetti, G., & Genoni, A. (2021). Climbing Jacob's Ladder of Structural Refinement: Introduction of a Localized Molecular orbital-Based Embedding for Accurate X-ray Determinations of Hydrogen Atom Positions. The journal of physical chemistry letters, 12(1), 463–471. https://doi.org/10.1021/acs.jpclett.0c03421

[75] Li, Y., Roy, A., & Zhang, Y. (2009). HAAD: A quick algorithm for accurate prediction of hydrogen atoms in protein structures. PloS one, 4(8), e6701. https://doi.org/10.1371/journal.pone.0006701

[76] Lee, M., Tan, L., Yang, H. et al. Structures of PPARγ complexed with lobeglitazone and pioglitazone reveal key determinants for the recognition of antidiabetic drugs. Sci Rep 7, 16837 (2017). https://doi.org/10.1038/s41598-017-17082-x

[77] Bhagwat, S. K., Patil, S. V., Vidal-Limon, A., Jimenez-Halla, J. o. C., Ghotekar, B. K., Bobade, V. D., Pérez-Landa, I. D., Delgado-Alvarado, E., Hernández-Rosas, F., & Pawar, T. J. (2025). Design and Evaluation of Indole-Based Schiff Bases as α-Glucosidase Inhibitors: CNN-Enhanced Docking, MD Simulations, ADMET Profiling, and SAR Analysis. Molecules (Basel, Switzerland), 30(17), 3651. https://doi.org/10.3390/molecules30173651

[78] Bieganski, R. M., & Yarmush, M. L. (2011). Novel ligands that target the mitochondrial membrane protein mitoNEET. Journal of molecular graphics & modelling, 29(7), 965–973. https://doi.org/10.1016/j.jmgm.2011.04.001

[79] Suh, D., Kim, G., & Im, W. (2026). CHARMM-GUI Ligand Docker for Molecular Docking with Various Docking Programs. Journal of chemical information and modeling, 66(7), 3416–3423. https://doi.org/10.1021/acs.jcim.6c00111

[80] Guo, W., Gao, S., Hao, Y., Li, Z., Hu, H., Wu, H., Hu, C., Cheng, X., Zhao, W., Kong, Y., Jiang, H., & Wang, S. (2025). Ultrasound-responsive diagnostic and therapeutic micro-/nanoplatforms for biomedical applications and clinical translation. Ultrasonics sonochemistry, 121, 107524. https://doi.org/10.1016/j.ultsonch.2025.107524

[81] Mosure, S. A., Shang, J., Eberhardt, J., Brust, R., Zheng, J., Griffin, P. R., Forli, S., & Kojetin, D. J. (2019). Structural Basis of Altered Potency and Efficacy Displayed by a Major in Vivo Metabolite of the Antidiabetic PPARγ Drug Pioglitazone. Journal of medicinal chemistry, 62(4), 2008–2023. https://doi.org/10.1021/acs.jmedchem.8b01573

[82] Gee, L. B., Pelmenschikov, V., Mons, C., Mishra, N., Wang, H., Yoda, Y., Tamasaku, K., Golinelli-Cohen, M.-P., & Cramer, S. P. (2021). NRVS and DFT of MitoNEET: Understanding the special vibrational structure of a [2Fe-2S] cluster with (Cys)3(His)1 ligation. Biochemistry, 60(31), 2419–2424. https://doi.org/10.1021/acs.biochem.1c00252

[83] Satheeshkumar, N., Shantikumar, S., & Srinivas, R. (2014). Pioglitazone: A review of analytical methods. Journal of Pharmaceutical Analysis, 4(5), 295–302. https://doi.org/10.1016/j.jpha.2014.02.002

[84] Ferecatu, I., Gonçalves, S., Golinelli-Cohen, M. P., Clémancey, M., Martelli, A., Riquier, S., Guittet, E., Latour, J. M., Puccio, H., Drapier, J. C., Lescop, E., & Bouton, C. (2014). The diabetes drug target MitoNEET governs a novel trafficking pathway to rebuild an Fe-S cluster into cytosolic aconitase/iron regulatory protein 1. The Journal of biological chemistry, 289(41), 28070–28086. https://doi.org/10.1074/jbc.M114.548438

[85] Pandey, A., Pain, J., Ghosh, A. K., Dancis, A., & Pain, D. (2015). Fe-S cluster biogenesis in isolated mammalian mitochondria: coordinated use of persulfide sulfur and iron and requirements for GTP, NADH, and ATP. The Journal of biological chemistry, 290(1), 640–657. https://doi.org/10.1074/jbc.M114.610402

[86] Lin, J., Zhou, T., Ye, K., & Wang, J. (2007). Crystal structure of human mitoNEET reveals distinct groups of iron sulfur proteins. *Proceedings of the National Academy of Sciences of the United States of America*, *104*(37), 14640–14645. https://doi.org/10.1073/pnas.0702426104

[87] Hoang, L. G., Goßen, J., Capelli, R., Nguyen, T. T., Sun, Z., Zuo, K., Schulz, J. B., Rossetti, G., & Carloni, P. (2022). Multiple Poses and Thermodynamics of Ligands Targeting Protein Surfaces: The Case of Furosemide Binding to mitoNEET in Aqueous Solution. *Frontiers in cell and developmental biology*, *10*, 886568. https://doi.org/10.3389/fcell.2022.886568

[88] Hoang LG, Goßen J, Capelli R, Nguyen TT, Sun Z, Zuo K, Schulz JB, Rossetti G and Carloni P (2022) Multiple Poses and Thermodynamics of Ligands Targeting Protein Surfaces: The Case of Furosemide Binding to mitoNEET in Aqueous Solution. Front. Cell Dev. Biol. 10:886568. doi: 10.3389/fcell.2022.886568

[89] Jakhar, R., Dangi, M., Khichi, A., & Chhillar, A. K. (2020). Relevance of molecular docking studies in drug designing. Current Bioinformatics, 15(4), 270–278. https://doi.org/10.2174/1574893615666191219094216

[90] Trott, o., & olson, A. J. (2010). AutoDock Vina: improving the speed and accuracy of docking with a new scoring function, efficient optimization, and multithreading. Journal of computational chemistry, 31(2), 455–461. https://doi.org/10.1002/jcc.21334

[91] Al Qumaizi, K. I., Anwer, R., Ahmad, N., Alosaimi, S. M., & Fatma, T. (2018). Study on the interaction of antidiabetic drug Pioglitazone with calf thymus DNA using spectroscopic techniques. Journal of molecular recognition : JMR, 31(11), e2735. https://doi.org/10.1002/jmr.2735

[92] Rossino, G., Rui, M., Pozzetti, L., Schepmann, D., Wünsch, B., Zampieri, D., Pellavio, G., Laforenza, U., Rinaldi, S., Colombo, G., Morelli, L., Linciano, P., Rossi, D., & Collina, S. (2020). Setup and Validation of a Reliable Docking Protocol for the Development of Neuroprotective Agents by Targeting the Sigma-1 Receptor (S1R). International journal of molecular sciences, 21(20), 7708. https://doi.org/10.3390/ijms21207708

[93] Chen, T., Shu, X., Zhou, H. et al. Algorithm selection for protein–ligand docking: strategies and analysis on ACE. Sci Rep 13, 8219 (2023). https://doi.org/10.1038/s41598-023-35132-5

[94] Hevener, K. E., Zhao, W., Ball, D. M., Babaoglu, K., Qi, J., White, S. W., & Lee, R. E. (2009). Validation of molecular docking programs for virtual screening against dihydropteroate synthase. Journal of chemical information and modeling, 49(2), 444–460. https://doi.org/10.1021/ci800293n

[98] Abbaoui, Z., Khibech, o., Karci, H., Dündar, M., Özdemir, İ., Gürbüz, N., Koç, A., Dino, W. A., Özdemir, İ., Alenazi, N., Touzani, R., & Alghibiwi, H. (2025). Synthesis, characterization, and anticancer evaluation of *N*-Heterocyclic entities: ADME profiling and *In Silico* predictions. *Toxicology reports*, *16*, 102184. https://doi.org/10.1016/j.toxrep.2025.102184

[99] Chung, T. D., Terry, D. B., & Smith, L. H. (2015). In vitro and in vivo assessment of ADME and PK properties during lead selection and lead optimization–guidelines, benchmarks and rules of thumb.

[97] Durán-Iturbide, N. A., Díaz-Eufracio, B. I., & Medina-Franco, J. L. (2020). In silico ADME/Tox profiling of natural products: A focus on BIoFACQUIM. *ACS omega, 5*(26), 16076–16084. https://doi.org/10.1021/acsomega.0c01581

[98] Banerjee, P., Eckert, A. o., Schrey, A. K., & Preissner, R. (2018). ProTox-II: a webserver for the prediction of toxicity of chemicals. Nucleic acids research, 46(W1), W257–W263. https://doi.org/10.1093/nar/gky318

[99] Kawaguchi-Suzuki, M., Cusi, K., Bril, F., Gong, Y., Langaee, T., & Frye, R. F. (2018). A Genetic Score Associates With Pioglitazone Response in Patients With Non-alcoholic Steatohepatitis. Frontiers in pharmacology, 9, 752. https://doi.org/10.3389/fphar.2018.00752

Chapter III

In Silico Tools and Software

III.1 Advanced Bioinformatics Toolsets for Protein-Ligand Characterization

The integration of computational methodologies into pharmaceutical research has revolutionized the identification and optimization of bioactive compounds. This chapter details the comprehensive suite of *in silico* web-based tools and specialized software utilized to evaluate the physicochemical, pharmacokinetic, and structural properties of the target molecules. These tools provide a systematic framework for predicting molecular behavior, binding affinities, and toxicological profiles, thereby streamlining the drug discovery pipeline [100].

III.2 In Silico Web-Based Tools

Web-based platforms offer accessible, high-performance computing resources for preliminary screening. These tools utilize sophisticated algorithms and extensive chemical libraries to provide predictive insights into molecular dynamics and biological interactions.

III.2.1 SwissADME: Pharmacokinetic and Drug-Likeness Assessment

SwissADME is an essential resource for assessing the Absorption, Distribution, Metabolism, and Excretion (ADME) parameters of small molecules. By inputting chemical structures, typically via SMILES notation, the tool generates a detailed profile of the molecule's "drug-likeness."

- **Physicochemical Descriptors**: The platform calculates fundamental properties such as molecular weight, topological polar surface area (TPSA), and hydrogen bond donors/acceptors. These parameters are critical for determining the solubility and permeability of a compound [101].
- **Lipophilicity and Solubility**: SwissADME utilizes five distinct models (iLoGP, XLoGP3, WLoGP, MLoGP, and SILICoS-IT) to estimate the partition coefficient, which influences a drug's ability to cross biological membranes.
- **The BoILED-Egg Model**: This unique visual tool predicts gastrointestinal absorption and blood-brain barrier (BBB) penetration by plotting the TPSA against the lipophilicity (WLoGP). This is crucial for determining if a compound can reach its intended therapeutic site [102].

- **Drug-Likeness Filters**: The software evaluates whether a molecule adheres to the Rule of Five (Lipinski), which identifies candidates likely to be orally active in humans [103].

- **Access URL**: http://www.swissadme.ch/

III.2.2 ProTox-3.0: Toxicological Profiling

ProTox-3.0 is a leading server for the in-silico prediction of oral toxicity and various toxicological endpoints. It serves as a vital gatekeeper in early-stage research by identifying potentially hazardous molecules before they progress to *in vitro* or *in vivo* testing.

- **Predictive Endpoints**: The tool estimates the median lethal dose (LD50) and classifies compounds into GHS (Globally Harmonized System) toxicity categories. It also screens for organ toxicity, such as hepatotoxicity, and adverse outcomes like mutagenicity or carcinogenicity [104].

- **Computational Basis**: ProTox-3.0 combines molecular similarity, machine learning models, and fragment-based rules to ensure high predictive accuracy based on a database of over 30,000 toxic and non-toxic compounds [105].

- **Access URL**: https://tox.charite.de/protox3/

III.2.3 RCSB Protein Data Bank (PDB)

The RCSB PDB is the authoritative global archive for the 3D structures of biological macromolecules. It provides the foundational structural data required for docking studies and molecular modeling.

- **Structural Retrieval**: High-resolution structures of targets, such as Bovine Serum Albumin (BSA), are retrieved from the PDB. These structures are typically determined via X-ray crystallography, NMR, or cryo-electron microscopy [106].

- **Validation**: Each entry includes validation reports that assess the quality of the experimental data, ensuring that the structural models used for *in silico* research are scientifically sound [107].

- **Access URL**: https://www.rcsb.org/

III.3 Computational Software Suites

Beyond web-based tools, specialized local software suites are employed for high-precision modeling, structure optimization, and molecular docking.

III.3.1 Gaussian 09 Computational Suite

Gaussian 09 is a comprehensive electronic structure program used by chemists, physicists, and engineers to predict the energies, molecular structures, and vibrational frequencies of molecular systems.

- **Electronic Structure Calculation**: It utilizes quantum mechanical equations to model the electronic properties of molecules. In this study, it serves as the primary engine for performing high-level calculations that go beyond classical mechanics to account for electronic transitions and bonding characteristics.
- **Geometry optimization**: Gaussian 09 is employed to perform energy minimization using various basis sets. By iteratively adjusting the coordinates of atoms, the software locates the global minimum on the Potential Energy Surface (PES), ensuring the structural inputs for docking are physically accurate and stable.
- **Molecular Property Prediction**: Beyond basic structure, the suite computes a wide array of molecular properties, including dipole moments, multipole moments, polarizability, and thermochemical data (such as enthalpy and Gibbs free energy).
- **Vibrational Analysis**: It is used to compute infrared (IR) and Raman spectra, as well as to verify that an optimized structure is a true local minimum (indicated by the absence of imaginary frequencies) rather than a transition state [108].
- **Access URL**: https://gaussian.com/g09citation/

III.3.2 MGLTools and AutoDock Vina

Molecular docking is the cornerstone of this structural analysis, and the combination of MGLTools and AutoDock Vina provides a highly efficient pipeline.

- **System Preparation (MGLTools)**: This suite is used to prepare the protein (receptor) and ligand files. It involves the addition of polar hydrogens, removal of water molecules, and

the assignment of Gasteiger charges, ultimately converting the files into the PDBQT format required for docking [109].

- **Docking Engine (AutoDock Vina)**: Vina uses a sophisticated scoring function and a global optimization algorithm to predict the binding affinity of a ligand to its target. It calculates the binding energy in kcal/mol, where a lower energy indicates a more stable and spontaneous binding event [110].

- **Access URL**: https://vina.scripps.edu/

III.3.3 Discovery Studio 2025 Client

BIoVIA Discovery Studio is a comprehensive software environment used for the visual analysis and refinement of molecular docking results.

- **Interaction Mapping**: It is primarily used to generate high-resolution 2D and 3D diagrams of ligand-protein complexes. This allows for a detailed inspection of the binding pocket and the specific amino acid residues involved in the interaction.

- **Surface Modeling**: The software can render the solvent-accessible surface area (SASA) and hydrophobicity maps, which are critical for assessing how a ligand fits within a target's cavity [111].

- **Access URL**: https://www.3dsbiovia.com/products/collaborative-science/biovia-discovery-studio/

III.3.4 ChemDraw: Chemical Structure Analysis

ChemDraw is the premier software for drawing, organizing, and analyzing chemical structures. It ensures that the chemical blueprints used throughout the study are structurally accurate.

- **Structural Accuracy**: It is used to generate precise 2D representations of ligands, ensuring proper stereochemistry and bond lengths.

- **Cheminformatics**: ChemDraw provides immediate data regarding molecular weight, exact mass, and estimated LogP. It also assists in identifying structural fragments that may contribute to biological activity or toxicity.

- **Isomeric Analysis**: The software is particularly useful for distinguishing between geometric isomers, which can exhibit vastly different pharmacological properties [112].
- **Access URL**: https://revvitysignals.com/products/research/chemdraw

References

[100] Lešnik, S., & Konc, J. (2020). In Silico Laboratory: Tools for Similarity-Based Drug Discovery. *Methods in molecular biology (Clifton, N.J.)*, *2089*, 1–28. https://doi.org/10.1007/978-1-0716-0163-1_1

[101] Xia X. (2017). Bioinformatics and Drug Discovery. *Current topics in medicinal chemistry*, *17*(15), 1709–1726. https://doi.org/10.2174/1568026617666161116143440

[102] Zhang, S., Liu, K., Liu, Y., Hu, X., & Gu, X. (2025). The role and application of bioinformatics techniques and tools in drug discovery. *Frontiers in pharmacology*, *16*, 1547131. https://doi.org/10.3389/fphar.2025.1547131

[103] Yu, W., Weber, D. J., & MacKerell, A. D., Jr (2023). Computer-Aided Drug Design: An Update. Methods in molecular biology (Clifton, N.J.), 2601, 123–152. https://doi.org/10.1007/978-1-0716-2855-3_7

[104] Banerjee, P., Kemmler, E., Dunkel, M., & Preissner, R. (2024). ProTox 3.0: a webserver for the prediction of toxicity of chemicals. Nucleic acids research, 52(W1), W513–W520. https://doi.org/10.1093/nar/gkae303

[105] Bittrich, S., Bhikadiya, C., Bi, C., Chao, H., Duarte, J. M., Dutta, S., Fayazi, M., Henry, J., Khokhriakov, I., Lowe, R., Piehl, D. W., Segura, J., Vallat, B., Voigt, M., Westbrook, J. D., Burley, S. K., & Rose, Y. (2023). RCSB Protein Data Bank: Efficient Searching and Simultaneous Access to one Million Computed Structure Models Alongside the PDB Structures Enabled by Architectural Advances. Journal of molecular biology, 435(14), 167994. https://doi.org/10.1016/j.jmb.2023.167994

[106] Burley, S. K., Berman, H. M., Christie, C., Duarte, J. M., Feng, Z., Westbrook, J., Young, J., & Zardecki, C. (2018). RCSB Protein Data Bank: Sustaining a living digital data resource that enables breakthroughs in scientific research and biomedical education. Protein science : a publication of the Protein Society, 27(1), 316–330. https://doi.org/10.1002/pro.3331

[107] Hiscocks, J., & Frisch, M. J. (2009). Gaussian 09: Iops Reference (pp. 1-170). M. Caricato, & M. J. Frisch (Eds.). Wallingford, CT, USA: Gaussian.

[108] Forli, S., Huey, R., Pique, M. E., Sanner, M. F., Goodsell, D. S., & olson, A. J. (2016). Computational protein-ligand docking and virtual drug screening with the AutoDock suite. Nature protocols, 11(5), 905–919. https://doi.org/10.1038/nprot.2016.051

[109] El-Hachem, N., Haibe-Kains, B., Khalil, A., Kobeissy, F. H., & Nemer, G. (2017). AutoDock and AutoDockTools for Protein-Ligand Docking: Beta-Site Amyloid Precursor Protein Cleaving Enzyme 1(BACE1) as a Case Study. Methods in molecular biology (Clifton, N.J.), 1598, 391–403. https://doi.org/10.1007/978-1-4939-6952-4_20

[110] Baroroh, U., Biotek, M., Muscifa, Z. S., Destiarani, W., Rohmatullah, F. G., & Yusuf, M. (2023). Molecular interaction analysis and visualization of protein-ligand docking using Biovia Discovery Studio Visualizer. Indonesian Journal of Computational Biology (IJCB), 2(1), 22-30.

[111] Cousins, K. R. (2005). ChemDraw Ultra 9.0. CambridgeSoft, 100 CambridgePark Drive, Cambridge, MA 02140. *Journal of the American Chemical Society, 127*(11), 4115–4116. https://doi.org/10.1021/ja0410237

[112] Li Z, Wan H, Shi Y, ouyang P. Personal experience with four kinds of chemical structure drawing software: review on ChemDraw, ChemWindow, ISIS/Draw, and ChemSketch. J Chem Inf Comput Sci. 2004 Sep-oct;44(5):1886-90. doi: 10.1021/ci049794h. PMID: 15446849.

Chapter IV

Results and Discussion

IV.1 Computational Analysis of MitoNEET Targeting

This chapter explores the therapeutic potential of Pioglitazone in comparison with the reference compound, furosemide, through molecular docking, ADME profiling, and toxicity assessments. By targeting the MitoNEET protein, the study evaluates how these compounds may disrupt cancer metabolism and modulate the Hexokinase II-associated metabolic pathway.

IV.1.1 Docking Validation

The validation of the molecular docking protocol represents a critical prerequisite for ensuring the reliability and reproducibility of computational binding predictions. In the present investigation, docking validation was performed through a redocking procedure using the crystallographic structure of the MitoNEET protein obtained from the Protein Data Bank under PDB ID: **6DE9**. The co-crystallized ligand was extracted from the native protein complex and subsequently reintroduced into the active binding pocket using the selected docking protocol in order to evaluate the ability of the computational method to accurately reproduce the experimentally determined binding orientation [113] .

The principal objective of redocking is to verify the structural precision of the docking algorithm and confirm that the adopted parameters are capable of reconstructing the native ligand pose within the active cavity. This process is particularly important for proteins such as MitoNEET, whose biological activity depends strongly on the integrity of its iron–sulfur coordination environment. MitoNEET belongs to the NEET family of iron-sulfur proteins and contains a highly sensitive [2Fe–2S] cluster that plays a fundamental role in mitochondrial redox regulation, oxidative metabolism, and electron transfer processes. Consequently, preservation of the structural arrangement surrounding the [2Fe–2S] center during docking simulations is essential for obtaining biologically meaningful interaction models.

The superimposition analysis between the docked ligand conformation and the crystallographic reference ligand demonstrated a high degree of structural overlap. The docked ligand, represented in orange, closely matched the experimentally resolved reference ligand shown in green, indicating that the docking procedure successfully reproduced the native orientation inside the MitoNEET binding pocket. The calculated root mean square deviation (RMSD) value was **1.896** Å, which

falls below the widely accepted validation threshold of 2.0 Å. RMSD values below this threshold are generally considered indicative of excellent docking reproducibility and reliable prediction of ligand-binding geometry [114].

From a structural perspective, the obtained RMSD value confirms that the selected docking methodology possesses adequate spatial accuracy for predicting ligand orientation within the active site of MitoNEET. The close overlap between the two conformations further suggests that the docking algorithm maintained the steric and electrostatic constraints governing ligand accommodation inside the receptor cavity. This observation is particularly significant because minor deviations in ligand positioning around the [2Fe–2S] cluster may profoundly influence predicted interaction energies and mechanistic interpretations.

The validation results therefore demonstrate that the adopted computational workflow provides a robust and reproducible framework for subsequent docking analyses involving Pioglitazone and Furosemide. Furthermore, the successful preservation of the native interaction environment reinforces the credibility of the calculated binding affinities and supports the reliability of the theoretical interaction models proposed in this study [115].

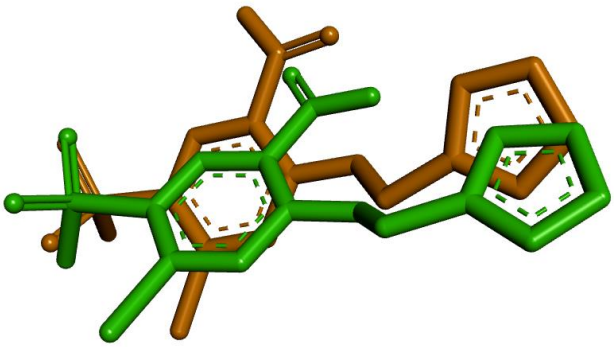

Figure 15: Docking validation of the co-crystallized ligand within the MitoNEET binding pocket (PDB: 6DE9) showing superimposition between **docked** and **reference conformations** with RMSD = 1.896 Å.

IV.1.2 Molecular Docking Analysis of Pioglitazone

The ball-and-stick model illustrates the 3D molecular structure of pioglitazone, optimized using Gaussian 09 software to highlight the conformational geometry of its thiazolidinedione ring and aromatic system.

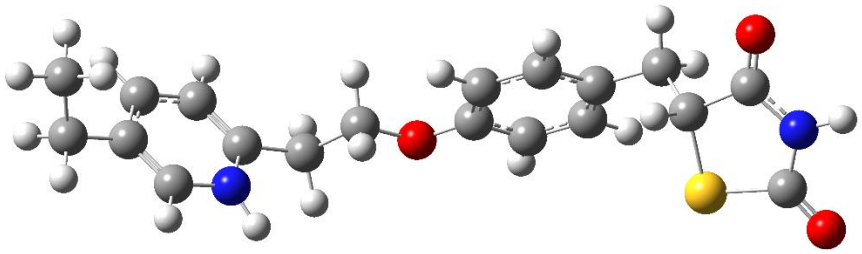

Figure 16: optimized Three-Dimensional (3D) Structure of Pioglitazone. Gray spheres represent carbon (C) atoms, red spheres represent oxygen (o) atoms, white spheres represent hydrogen (H) atoms, blue spheres represent nitrogen (N) atoms, and yellow spheres repre

The molecular docking investigation of Pioglitazone against MitoNEET revealed a highly favorable binding profile, suggesting substantial ligand affinity toward the mitochondrial target protein. The calculated free binding energy (3.34×10^6, accompanied by a binding constant of 3.7×10^5, indicating the spontaneous formation of a stable ligand–protein complex under thermodynamically favorable conditions.

The negative Gibbs free energy value reflects an energetically advantageous interaction process, implying that Pioglitazone can be accommodated efficiently within the MitoNEET active cavity. In molecular docking studies, increasingly negative **ΔG values** are generally associated with stronger intermolecular interactions, improved complex stability, and enhanced residence time within the binding site. The magnitude of the observed binding energy therefore suggests a significant interaction potential between Pioglitazone and **MitoNEET**.

The relatively elevated binding constant further supports the hypothesis of strong ligand association. Binding constants in the range of 10^5 commonly indicate stable molecular recognition driven by a combination of hydrogen bonding, hydrophobic interactions, van der Waals

stabilization, and electrostatic complementarity. Considering the amphipathic structure of Pioglitazone, its thiazolidinedione scaffold may contribute substantially to receptor stabilization through polar interactions with amino acid residues located near the iron-sulfur coordination environment.

The docking pose additionally suggests that Pioglitazone occupies the active pocket in a geometrically favorable orientation capable of maximizing intermolecular contact surface area. Such structural accommodation may facilitate stabilization of the ligand within the mitochondrial binding cavity and potentially interfere with the physiological redox functions of MitoNEET. Since **MitoNEET** regulates mitochondrial oxidative balance and iron-sulfur cluster transfer, ligand binding could perturb mitochondrial electron transport dynamics and alter reactive oxygen species (RoS) homeostasis.

The biological implications of this interaction are particularly relevant in **cancer metabolism**. MitoNEET has been implicated in the regulation of mitochondrial bioenergetics, metabolic plasticity, and tumor cell survival. Cancer cells frequently rely on adaptive mitochondrial signaling pathways to sustain proliferation and resist apoptosis. Therefore, pharmacological disruption of MitoNEET function may impair mitochondrial integrity, increase oxidative stress, and sensitize malignant cells to apoptosis induction [116] .

Moreover, the thiazolidinedione scaffold of **Pioglitazone** has attracted increasing attention in drug repurposing research due to its reported influence on mitochondrial signaling pathways and metabolic modulation. Although originally developed as an insulin-sensitizing agent, Pioglitazone has demonstrated potential anti-proliferative properties in several cancer-related investigations. The present docking findings support the hypothesis that these effects may partially involve direct interaction with mitochondrial regulatory proteins such as **MitoNEET** [117-118] .

Table 1: Molecular docking parameters of Pioglitazone against MitoNEET receptor.

Compound	Target Protein	ΔG (kJ/mol)	Binding Constant (K)	Interpretation

Pioglitazone	MitoNEET (6DE9)	−31.8	3.7×10^5	Strong and thermodynamically favorable ligand–protein interaction with high predicted stability

The following figure illustrates the molecular docking results, highlighting the binding orientation of the ligand within the protein's active pocket. The expanded view details specific intermolecular interactions, such as hydrogen bonds and hydrophobic contacts, essential for stabilizing the complex and evaluating binding affinity.

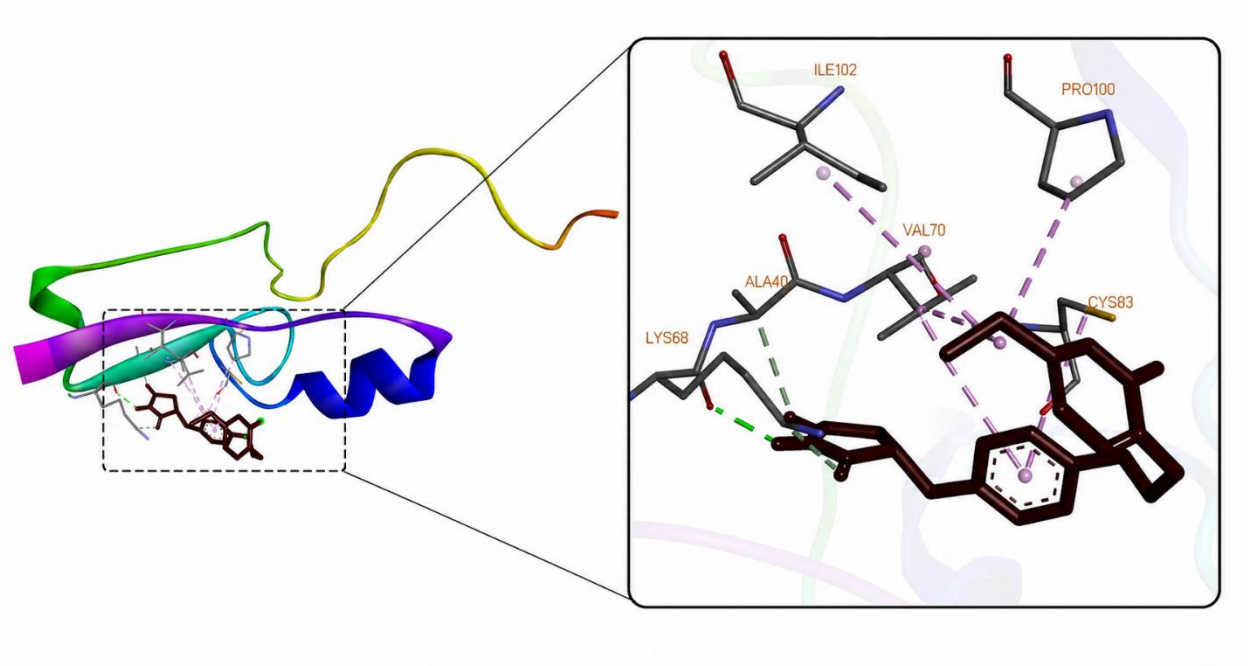

Figure 17: Predicted docking pose of Pioglitazone inside the active site of MitoNEET protein.

IV.1.3 Molecular Docking Analysis of Furosemide

The docking analysis of Furosemide against the MitoNEET receptor demonstrated favorable but comparatively weaker binding characteristics relative to Pioglitazone. The calculated binding free energy was **−26.4 kJ/mol**, while the corresponding binding constant reached **4.2×10^4**, indicating spontaneous ligand association with the receptor but with reduced interaction strength.

The negative ΔG value confirms that Furosemide can establish energetically favorable interactions within the active cavity of **MitoNEET**. However, the less negative binding energy compared with Pioglitazone suggests lower thermodynamic stability of the resulting **complex**. This difference may reflect variations in structural complementarity, interaction geometry, or intermolecular contact efficiency within the **receptor pocket**.

Similarly, the lower binding constant indicates weaker ligand retention and potentially shorter residence time inside the binding cavity. Reduced binding stability may limit the ability of **Furosemide** to sustain prolonged modulation of **MitoNEET**-associated mitochondrial processes. Nevertheless, the observed affinity still supports the possibility of biologically relevant interaction with the **target protein**.

The docking orientation of **Furosemide** suggests partial accommodation inside the active cavity with the potential formation of hydrogen bonds and electrostatic interactions mediated by its sulfonamide and carboxyl functional groups. Despite these **favorable interactions**, the molecular conformation of Furosemide may not optimize hydrophobic packing to the same extent as Pioglitazone. Consequently, the interaction network appears comparatively **less stable**.

From a pharmacological perspective, **Furosemide** remains an interesting reference compound due to its reported effects on cellular ionic balance and metabolic regulation. However, the docking results indicate that its affinity toward **MitoNEET** is substantially lower than that observed for Pioglitazone. This difference suggests that Pioglitazone may possess superior capacity for mitochondrial targeting and modulation of redox-associated **signaling pathways**.

The **weaker interaction** profile of Furosemide also has implications for drug repurposing suitability. Effective repurposed anti-cancer agents generally require sufficient **target affinity** to induce meaningful biological modulation at therapeutically achievable concentrations. Although **Furosemide** exhibits acceptable binding behavior, the computational data suggest that its mitochondrial interaction efficiency may be comparatively limited [119].

Table 2: Molecular docking parameters of Furosemide against MitoNEET receptor.

Compound	Target Protein	ΔG (kJ/mol)	Binding Constant (K)	Interpretation
Furosemide	MitoNEET (6DE9)	−26.4	4.2×10^4	Moderately favorable interaction with lower predicted complex stability

The following scientific visualization illustrates the molecular docking of a high-affinity ligand within a protein's binding pocket. The transition from a global ribbon structure to a detailed atomistic view highlights the specific non-covalent interactions, including hydrogen bonds, that stabilize the complex.

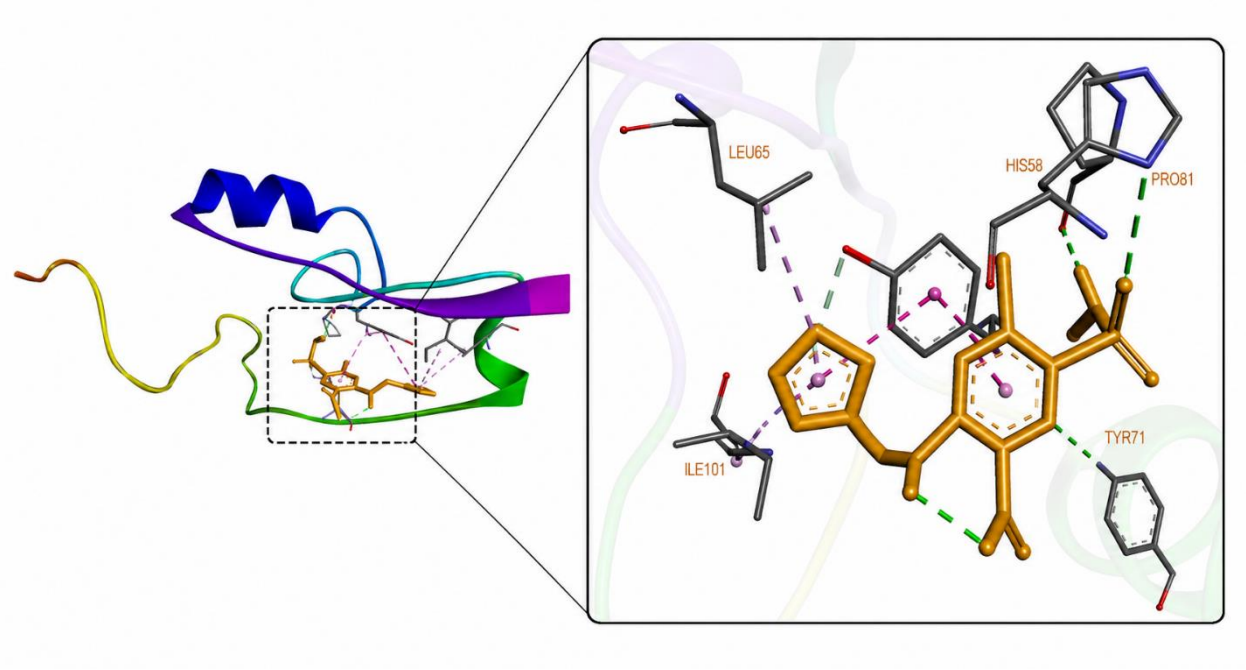

Figure 18: Predicted docking pose of Furosemide inside the MitoNEET binding cavity.

IV.1.4 Comparative Interpretation of Docking Results

Comparative evaluation of the docking findings revealed substantial differences between Pioglitazone and **Furosemide** regarding their predicted interaction behavior with **MitoNEET**. Among the investigated compounds, **Pioglitazone** demonstrated the strongest binding affinity, as evidenced by its more negative binding free energy and significantly higher **binding constant**.

The approximately **5.4 kJ/mol** difference in ΔG values between the two ligands indicates that Pioglitazone forms a thermodynamically more stable receptor complex. Since free energy values reflect the balance between stabilizing and destabilizing intermolecular forces, the enhanced affinity of **Pioglitazone** likely arises from improved geometric complementarity and more extensive interaction networks inside the **receptor cavity**.

The markedly higher binding constant observed for **Pioglitazone** further reinforces this interpretation. Stronger ligand association generally correlates with improved target occupancy and increased probability of biologically relevant modulation. In the context of mitochondrial proteins such as **MitoNEET**, sustained target engagement may be essential for altering mitochondrial redox signaling and disrupting cancer-associated metabolic adaptation.

Differences in structural scaffolds may also contribute significantly to the observed interaction disparity. The thiazolidinedione nucleus of **Pioglitazone** provides a favorable balance between hydrophobic and polar interaction capacity, potentially enhancing receptor stabilization near the [2Fe–2S] regulatory region. In contrast, the comparatively rigid and polar architecture of Furosemide may limit optimal accommodation within hydrophobic segments of the **binding pocket.**

From a drug repurposing perspective, the superior interaction profile of **Pioglitazone** suggests greater potential for mitochondrial-targeted anti-cancer applications. **MitoNEET** has emerged as a promising therapeutic target because of its involvement in mitochondrial homeostasis, RoS regulation, and tumor metabolic adaptation. Ligands capable of strongly interacting with this protein may interfere with mitochondrial function sufficiently to induce oxidative stress and apoptosis in **malignant cells**.

Despite the promising theoretical findings, it is important to acknowledge the inherent limitations of computational docking studies. **Binding affinities** derived from docking simulations represent predictive approximations rather than experimentally confirmed interaction energies. Therefore, additional molecular dynamics simulations, biochemical assays, and cellular validation studies remain necessary to confirm the stability and biological relevance of the predicted **complexes** [120].

Table 3: Comparative molecular docking analysis of investigated compounds against MitoNEET.

Compound	ΔG (kJ/mol)	Binding Constant	Relative Affinity	Predicted Stability
Pioglitazone	−31.8	3.7×10^5	High	Strong
Furosemide	−26.4	4.2×10^4	Moderate	Intermediate

IV.2 In Silico ADME Investigation

The pharmacokinetic suitability of repurposed drug candidates represents a critical determinant of therapeutic applicability. In this study, in silico ADME analysis was performed to evaluate the physicochemical and pharmacokinetic characteristics of Pioglitazone and Furosemide, with particular emphasis on parameters influencing oral bioavailability, membrane permeability, and systemic distribution.

Table 4: SMILES codes of Bioglitazone and Furosemide

Sample	SMILES Code
Bioglitazone	CCC1=CN=C(C=C1)CCoC2=CC=C(C=C2)CC3C(=o)NC(=o)S3
Furosemide	C1=CoC(=C1)CNC2=CC(=C(C=C2C(=O)o)S(=o)(=o)N)Cl

Pioglitazone exhibited a molecular weight of **356.44 g/mol**, which remains within the acceptable range proposed by Lipinski's rule of five. Its calculated **logP** value of **3.49** indicates moderate lipophilicity, suggesting favorable balance between aqueous solubility and membrane permeability. Molecules within this lipophilicity range generally demonstrate efficient passive diffusion across biological membranes, including mitochondrial membranes characterized by **high phospholipid content**.

The topological polar surface area (**TPSA**) of Pioglitazone was calculated at **93.59 Å²**, a value compatible with satisfactory intestinal absorption and oral bioavailability. Additionally, the presence of six hydrogen bond acceptors and one hydrogen bond donor suggest adequate capacity for receptor interaction without excessive polarity that could impair membrane penetration. The seven rotatable bonds further indicate moderate molecular flexibility, which may facilitate adaptive conformational fitting inside **protein binding cavities**.

In contrast, Furosemide demonstrated a molecular weight of **330.74 g/mol** and a slightly higher **logP** value of 3.74, reflecting comparable lipophilic behavior. However, its substantially elevated **TPSA** value of **131.01 Å²** suggests increased polarity, which may reduce passive membrane permeability and limit intracellular diffusion efficiency. The presence of three hydrogen bond donors may additionally enhance intermolecular interactions with aqueous environments, potentially decreasing membrane transit capacity.

Although both compounds generally satisfy major drug-likeness criteria, **Pioglitazone** appears to possess a more favorable pharmacokinetic balance for mitochondrial targeting applications. Its lower **TPSA** and controlled hydrogen-bonding profile likely support improved permeability through cellular and mitochondrial membranes. Since **MitoNEET** is localized within the outer mitochondrial membrane, efficient intracellular distribution represents an important prerequisite for **pharmacological activity**.

The ADME findings therefore reinforce the docking observations by suggesting that Pioglitazone combines strong target affinity with favorable pharmacokinetic properties. Such integration of binding efficiency and membrane permeability constitutes an important advantage in computational drug repurposing strategies aimed at intracellular mitochondrial targets [121-122].

Table 5: Physicochemical and **ADME**-related properties of investigated compounds.

Property	Recommended Value	Pioglitazone	Furosemide
Molecular Weight (g/mol)	**≤ 500**	356.44	330.74
H-Bond Acceptors	**≤ 10**	6	6
H-Bond Donors	**≤ 5**	1	3
Rotatable Bonds	**≤ 10**	7	5
TPSA (Å²)	**< 140 Å²**	93.59	131.01
logP	**≤ 5**	3.49	3.74
Predicted Membrane Permeability	**Favorable**	Favorable	Moderate
Oral Bioavailability Prediction	**Good**	Good	Acceptable
Overall Drug-Likeness	**Favorable**	Favorable	Moderately Favorable

IV.3 In Silico Toxicity Profiling

Toxicological prediction constitutes a crucial component of computational drug repurposing workflows because therapeutic efficacy must be balanced against systemic safety. In the present investigation, toxicity assessment was conducted using ProTox-3.0 to evaluate the predicted toxicological behavior of Pioglitazone and Furosemide, including acute toxicity, organ-specific adverse effects, metabolic interactions, and stress-response signaling pathways [123].

IV.3.1 Toxicity Profile of Pioglitazone

The predicted oral **LD50** value for Pioglitazone was **1000 mg/kg**, corresponding to Toxicity Class 4. This classification indicates moderate acute toxicity according to globally accepted toxicological standards. Although not considered highly toxic, compounds within this category require controlled therapeutic administration and **monitoring during long-term clinical use**.

The **hepatotoxicity** prediction was classified as active, suggesting a potential risk of hepatic stress or liver-associated adverse effects. This observation aligns with known concerns regarding thiazolidinedione-mediated hepatic metabolism and highlights the importance of **liver function** monitoring during therapeutic application. In oncology settings, where patients frequently receive multidrug regimens, hepatic monitoring becomes particularly relevant due to the increased probability of cumulative **metabolic burden**.

Cardiotoxicity prediction was classified as inactive, indicating a relatively low probability of direct cardiac adverse effects. This finding is favorable for potential anti-cancer repurposing because cardiotoxicity remains a major limitation for many conventional chemotherapeutic agents.

The **CYP450** interaction analysis demonstrated active interaction with **CYP2C9** but inactive behavior toward **CYP3A4**. **CYP2C9** involvement suggests potential susceptibility to drug–drug interactions, especially in patients receiving co-administered medications metabolized through the same enzymatic pathway. Such interactions may influence plasma drug concentration, therapeutic efficacy, and toxicity profiles.

Interestingly, Pioglitazone demonstrated inactive predictions for both mitochondrial membrane potential disruption (sr_mmp) and **p53** stress-response signaling (sr_p53). The absence of predicted mitochondrial membrane destabilization may indicate selective mitochondrial modulation rather than generalized mitochondrial toxicity. Similarly, inactive **p53** stress signaling suggests that the compound may not induce severe genotoxic stress under predicted exposure conditions.

Collectively, the toxicity profile of Pioglitazone supports its potential repositioning as a mitochondrial-targeted therapeutic candidate while simultaneously emphasizing the necessity for hepatic safety evaluation in future **experimental studies**.

Table 6: Predicted toxicity profile of Pioglitazone using ProTox-3.0.

Parameter	Prediction	Probability	Interpretation
LD50	1000 mg/kg		Indicates moderate acute oral toxicity with an estimated lethal dose of 1000 mg/kg.
Toxicity Class	**4**		Falls within GHS Toxicity Class 4, suggesting harmful effects if swallowed at relatively high doses.
Hepatotoxicity	**Active**	0.70	Predicted potential to induce liver toxicity or hepatic stress.
Cardiotoxicity	**Inactive**	0.74	No significant likelihood of causing toxic effects on cardiac tissue.
CYP2C9	**Active**	0.68	Likely to interact with or inhibit the CYP2C9 metabolic enzyme pathway.
CYP3A4	**Inactive**	0.73	Unlikely to significantly affect CYP3A4-mediated metabolism.
sr_mmp	**Inactive**	0.76	No predicted disruption of mitochondrial membrane potential.
sr_p53	**Inactive**	0.79	Unlikely to activate p53 stress-response or DNA-damage signaling pathways.

IV.3.2 Toxicity Profile of Furosemide

The predicted toxicity profile of Furosemide revealed an ***LD50*** value of **2000 mg/kg**, corresponding to **Toxicity Class 4**. Compared with Pioglitazone, the higher **LD50** value suggests lower predicted acute systemic toxicity and a comparatively broader safety margin.

Both hepatotoxicity and cardiotoxicity predictions were classified as inactive, indicating reduced probability of major hepatic or cardiac adverse effects. This relatively favorable organ toxicity profile may represent an advantage in clinical settings involving prolonged administration or multidrug therapeutic combinations.

In addition, both **CYP2C9** and **CYP3A4** predictions were inactive, suggesting a lower likelihood of clinically significant metabolic drug–drug interactions. Reduced **CYP450** involvement may contribute to greater pharmacokinetic stability and simplified therapeutic management.

Despite its comparatively safer toxicological profile, the weaker docking affinity of **Furosemide** remains a limiting factor regarding its theoretical anti-cancer efficacy through **MitoNEET** targeting. Therefore, while Furosemide may offer improved systemic tolerability, its reduced predicted interaction strength may compromise target modulation efficiency.

Table 7: Predicted toxicity profile of Furosemide using ProTox-3.0.

Parameter	Prediction	Probability	Interpretation
LD50	2000 mg/kg		Indicates moderate acute toxicity with an estimated median lethal dose of 2000 mg/kg.
Toxicity Class	**4**		Classified as Toxicity Class 4 according to the Globally Harmonized System (GHS), suggesting low-to-moderate toxicity risk.
Hepatotoxicity	**Inactive**	0.59	The compound is predicted to have no significant liver toxicity potential, with moderate confidence.
Cardiotoxicity	**Inactive**	0.72	Predicted to be non-cardiotoxic, indicating a relatively low risk of adverse cardiac effects with good confidence.
CYP2C9	**Inactive**	0.57	Suggests the compound is unlikely to inhibit or significantly interact with the CYP2C9 metabolic enzyme.
CYP3A4	**Inactive**	0.64	Indicates a low probability of interaction or inhibition of the CYP3A4 enzyme involved in drug metabolism.

IV.4 Mechanistic Interpretation of MitoNEET Targeting

MitoNEET is a mitochondrial outer membrane protein belonging to the NEET family of iron–sulfur cluster-containing proteins that participate in **redox regulation** and mitochondrial metabolic homeostasis. Its biological significance derives primarily from its capacity to coordinate and transfer **[2Fe–2S]** clusters involved in electron transport, oxidative phosphorylation, and cellular stress adaptation.

Cancer cells exhibit profound metabolic reprogramming characterized by altered mitochondrial dynamics, increased oxidative stress tolerance, and enhanced metabolic flexibility. **MitoNEET** contributes to these adaptive processes by regulating mitochondrial iron homeostasis and RoS balance. overexpression of **MitoNEET** has been associated with enhanced tumor cell survival, metabolic plasticity, and resistance to apoptosis.

Targeting **MitoNEET** therefore represents a potentially valuable anti-cancer strategy because interference with iron–sulfur cluster regulation may destabilize mitochondrial bioenergetics and promote oxidative stress accumulation. **Excessive RoS generation** can induce mitochondrial dysfunction, lipid peroxidation, DNA damage, and activation of **apoptotic signaling pathways**.

The docking findings obtained in the present study suggest that **Pioglitazone** may effectively associate with the **MitoNEET** binding cavity and potentially interfere with its regulatory function. Strong ligand binding near the **[2Fe–2S]** coordination environment could alter electron transfer efficiency and disrupt mitochondrial redox equilibrium. Such perturbation may sensitize cancer cells to oxidative injury and reduce their **adaptive metabolic capacity**.

Interestingly, the inactive mitochondrial membrane potential prediction observed for **Pioglitazone** suggests that the compound may modulate mitochondrial signaling without inducing indiscriminate mitochondrial collapse. This distinction is important because selective mitochondrial stress induction may provide anti-cancer activity while minimizing nonspecific cytotoxicity toward **normal cells**.

overall, the mechanistic findings support the hypothesis that **Pioglitazone** may exert anti-cancer effects partially through mitochondrial targeting and modulation of **MitoNEET**-associated metabolic pathways. However, experimental validation remains essential to confirm whether the

predicted computational interactions translate into measurable biological activity in cellular and in vivo systems [124].

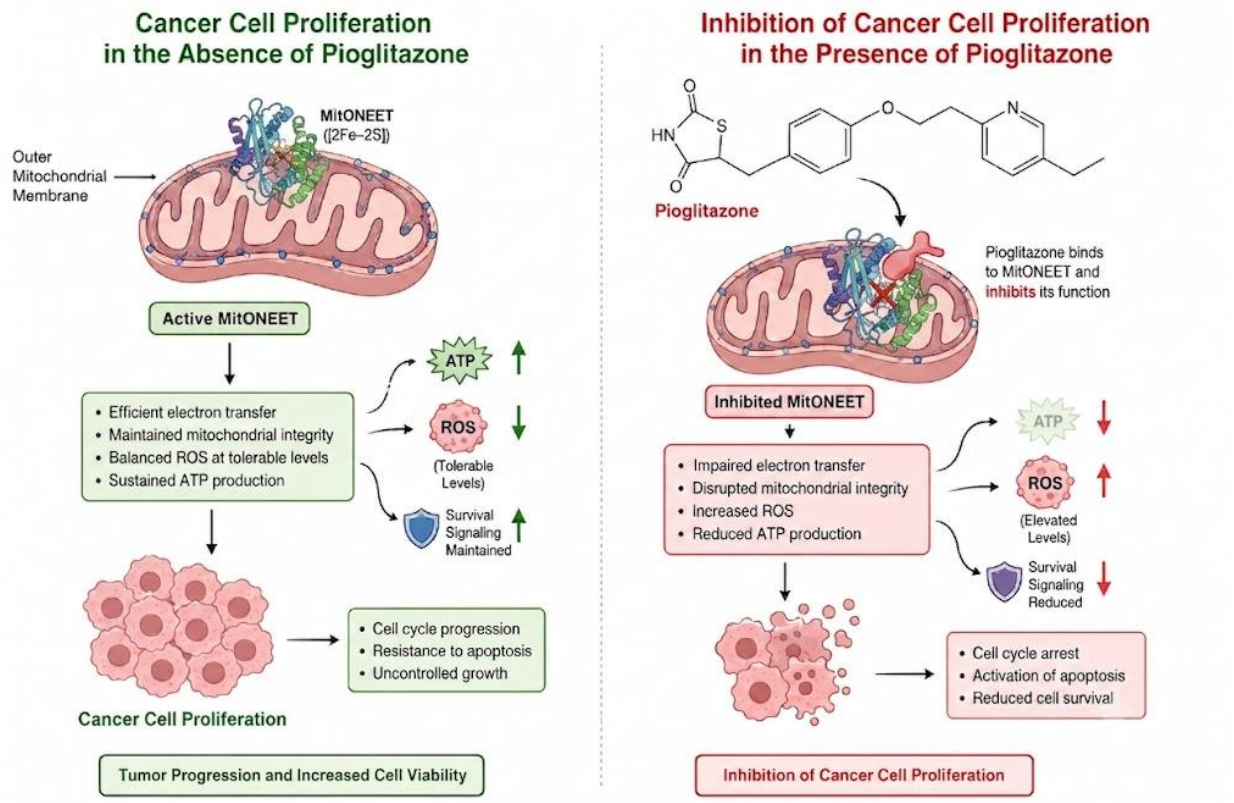

Figure 19: Schematic illustration of cancer cell proliferation pathways in the absence (**eft**) and presence (**right**) of pioglitazone, highlighting mitochondrial dysfunction induced by mitoNEET inhibition.

Applying the General Objective and Covering the Research Gap

In alignment with the primary objective of this investigation, the computational findings presented herein successfully evaluate the therapeutic potential of pioglitazone as a selective inhibitor of cancer-associated Hexokinase II (Its function was indirectly inhibited by creating a disruption in the role of mitoNEET as a result of its binding to pioglitazone), thereby establishing a robust molecular foundation for its repurposing in oncology. Prior to this study, a significant gap persisted in the literature regarding the precise structural interactions of pioglitazone with Hexokinase II, leaving its efficacy as a repurposed anticancer agent largely uncharacterized. This research directly addresses this deficiency through a systematic, integrated in silico framework.

By combining advanced molecular optimization, targeted molecular docking simulations, and detailed binding interaction visualizations, this work explicitly maps the geometric and energetic affinities of the pioglitazone-receptor complex. Furthermore, the correlation of these binding dynamics with comprehensive ADME assessments and toxicity predictions provides a complete pharmacokinetic profile that justifies its safety and viability. Consequently, these integrated computational results not only resolve the existing ambiguity surrounding the molecule's targeted antineoplastic mechanisms but also validate the broader strategic objective of leveraging established therapeutics to accelerate drug discovery in cancer research.

IV.5 Overall Scientific Conclusion of the Results

This computational study investigated the potential of **Pioglitazone** as a repurposed anti-cancer agent targeting the mitochondrial protein **MitoNEET** to indirectly modulate **Hexokinase II**. **Furosemide** was included solely as a comparative reference compound. Docking validation confirmed the reliability of the computational protocol, with an **RMSD** value of **1.896 Å** indicating accurate ligand positioning within the active site. Pioglitazone demonstrated the strongest receptor interaction, showing favorable binding energy (**ΔG = −31.8 kJ/mol**) and high binding stability, whereas **Furosemide** exhibited weaker affinity.

The findings are significant because **MitoNEET** plays a critical role in mitochondrial redox regulation and metabolic adaptation, processes closely linked to Hexokinase II-dependent tumor metabolism and the Warburg effect. Strong binding of Pioglitazone to **MitoNEET** suggests a possible mechanism for disrupting mitochondrial homeostasis, increasing oxidative stress, and impairing cancer cell survival. **ADME** analysis further supported Pioglitazone’s therapeutic potential by revealing favorable pharmacokinetic properties and membrane permeability compatible with mitochondrial targeting. Toxicity predictions indicated moderate systemic and hepatic risks but no major cardiotoxicity. overall, the integrated computational results support Pioglitazone as a promising mitochondrial-targeted anti-cancer candidate requiring further **experimental validation**

References

[113] omar AM, Aljahdali AS, Safo MK, Mohamed GA, Ibrahim SRM. Docking and Molecular Dynamic Investigations of Phenylspirodrimanes as Cannabinoid Receptor-2 Agonists. Molecules. 2022 Dec 21;28(1):44. doi: 10.3390/molecules28010044. PMID: 36615238; PMCID: PMC9821895.

[114] Kirchmair, J., Markt, P., Distinto, S. *et al.* Evaluation of the performance of 3D virtual screening protocols: RMSD comparisons, enrichment assessments, and decoy selection—What can we learn from earlier mistakes?. *J Comput Aided Mol Des* **22**, 213–228 (2008). https://doi.org/10.1007/s10822-007-9163-6

[115] Geldenhuys, W. J., Leeper, T. C., & Carroll, R. T. (2014). mitoNEET as a novel drug target for mitochondrial dysfunction. *Drug Discovery Today*, *19*(10), 1601–1606. https://doi.org/10.1016/j.drudis.2014.05.001

[116] Song, G., Tian, F., Liu, H., Li, G., & Zheng, P. (2021). Pioglitazone inhibits metal cluster transfer of mitoNEET by stabilizing the labile Fe–N bond revealed at single-bond level. *The Journal of Physical Chemistry Letters*, *12*(15), 3860–3867. https://doi.org/10.1021/acs.jpclett.0c03852

[117] Salem AF, Whitaker-Menezes D, Howell A, Sotgia F, Lisanti MP. Mitochondrial biogenesis in epithelial cancer cells promotes breast cancer tumor growth and confers autophagy resistance. Cell Cycle. 2012 Nov 15;11(22):4174-80. doi: 10.4161/cc.22376. Epub 2012 oct 15. PMID: 23070475; PMCID: PMC3524213.

[118] Ninomiya I, Yamazaki K, oyama K, Hayashi H, Tajima H, Kitagawa H, Fushida S, Fujimura T, ohta T. Pioglitazone inhibits the proliferation and metastasis of human pancreatic cancer cells. oncol Lett. 2014 Dec;8(6):2709-2714. doi: 10.3892/ol.2014.2553. Epub 2014 Sep 23. PMID: 25364454; PMCID: PMC4214501.

[119] Harras, M. F., Sabour, R., Farghaly, T. A., & Ibrahim, M. H. (2023). Drug repurposing approach in developing new furosemide analogs as antimicrobial candidates and anti-PBP: Design, synthesis, and molecular docking. *Bioorganic Chemistry*, *137*, 106585. https://doi.org/10.1016/j.bioorg.2023.106585

[120] F. Bai, F. Morcos, Y. Sohn, M. Darash-Yahana, C.o. Rezende, C.H. Lipper, M.L. Paddock, L. Song, Y. Luo, S.H. Holt, S. Tamir, E.A. Theodorakis, P.A. Jennings, J.N. onuchic, R. Mittler, & R. Nechushtai, The Fe-S cluster-containing NEET proteins mitoNEET and NAF-1 as chemotherapeutic targets in breast cancer, Proc. Natl. Acad. Sci. U.S.A. 112 (12) 3698-3703, https://doi.org/10.1073/pnas.1502960112 (2015).

[121] Hubbard WB, Spry ML, Gooch JL, Cloud AL, Vekaria HJ, Burden S, Powell DK, Berkowitz BA, Geldenhuys WJ, Harris NG, Sullivan PG. Clinically relevant mitochondrial-targeted therapy improves chronic outcomes after traumatic brain injury. Brain. 2021 Dec 31;144(12):3788-3807. doi: 10.1093/brain/awab341.PMID: 34972207; PMCID: PMC8719838.

[122] Sauerbeck A, Gao J, Readnower R, Liu M, Pauly JR, Bing G, Sullivan PG. Pioglitazone attenuates mitochondrial dysfunction, cognitive impairment, cortical tissue loss, and inflammation following traumatic brain injury. Exp Neurol. 2011 Jan;227(1):128-35. doi: 10.1016/j.expneurol.2010.10.003.Epub 2010 oct 20. PMID: 20965168; PMCID: PMC3019268.

[123] Banerjee P, Kemmler E, Dunkel M, Preissner R. ProTox 3.0: a webserver for the prediction of toxicity of chemicals. Nucleic Acids Res. 2024 Jul 5;52(W1):W513-W520. doi: 10.1093/nar/gkae303.PMID: 38647086; PMCID: PMC11223834.

[124] Singh, A., Faccenda, D., & Campanella, M. (2021). Pharmacological advances in mitochondrial therapy. *EBioMedicine*, *65*, 103244. https://doi.org/10.1016/j.ebiom.2021.103244

Conclusion

The research successfully utilized a computational modeling and therapeutic drug repurposing framework to investigate whether Pioglitazone, a common drug approved for Type 2 diabetes, can act as an indirect anti-cancer agent. Rather than creating a new drug from scratch, the study targets the metabolic vulnerabilities of cancer cells specifically the Warburg Effect, where cancer cells prioritize accelerated glycolysis for rapid proliferation.

Cancer cells achieve rapid growth and apoptotic resistance by physically anchoring the enzyme Hexokinase II (HKII) to the outer mitochondrial membrane via the Voltage-Dependent Anion Channel (VDAC), giving HKII direct, preferential access to newly synthesized mitochondrial ATP. This thesis explores disrupting this microenvironment by computationally targeting MitoNEET (CISD1), an outer mitochondrial membrane protein responsible for iron-sulfur [2Fe-2S] cluster transfer, redox sensing, and metabolic homeostasis.

Molecular docking simulations (validated with an accurate RMSD of 1.896 Å) demonstrated that Pioglitazone exhibits strong receptor interaction with MitoNEET, achieving a favorable binding energy (ΔG = -31.8 kJ/mol) and high binding stability. Pioglitazone vastly outperformed the reference compound, Furosemide, showing a ~5.4 kJ/mol advantage in binding free energy due to the better geometric complementarity of Pioglitazone's thiazolidinedione (TZD) core scaffold within the receptor cavity. This strong binding near MitoNEET's [2Fe-2S] centers suggests that Pioglitazone can destabilize mitochondrial bioenergetics, increase toxic oxidative stress (RoS), and impair the metabolic adaptation that feeds cancer cell survival.

Additionally, in silico pharmacokinetic testing (via SwissADME and BoILED-Egg mapping) confirmed that Pioglitazone possesses excellent drug-likeness, obeying Lipinski's Rule of Five, and demonstrates good membrane permeability necessary to reach mitochondrial targets. Toxicological profiling (via ProTox platforms) indicates that Pioglitazone does not induce indiscriminate mitochondrial collapse, implying it can selectively stress cancer metabolism while minimizing nonspecific toxicities to healthy tissues.

Altogether, the computational data strongly supports the hypothesis that Pioglitazone can be repurposed as an effective anti-cancer therapeutic. By tightly binding to MitoNEET, it presents a viable pathway to disrupt mitochondrial homeostasis, indirectly suppress HKII-driven tumor metabolism, and overcome cancer cell resistance.

Abstract

Cancer cells undergo a metabolic shift (the Warburg effect) that prioritizes rapid glycolysis over oxidative phosphorylation, heavily driven by the overexpression of Hexokinase II (HKII) anchored to the outer mitochondrial membrane. Because de novo drug development is resource-intensive, drug repurposing offers an accelerated therapeutic alternative. Pioglitazone, an approved anti-diabetic thiazolidinedione, exhibits off-target anti-cancer properties by directly interacting with mitoNEET (CISD1), an outer mitochondrial iron-sulfur [2Fe-2S] cluster protein essential for cellular bioenergetics.

This study uses integrated *in silico* computational approaches to evaluate the potential of pioglitazone as an indirect metabolic inhibitor of cancer-associated HKII via mitoNEET targeting.

The 3D crystal structure of human mitoNEET (PDB ID: 6DE9) was prepared and subjected to site-directed molecular docking simulations using AutoDock Vina, with protocol accuracy validated at an RMSD threshold of 1.896 Å. Computational outcomes were comparatively benchmarked against Furosemide, a known mitoNEET modulator. Pharmacoinformatics (*in silico* ADME) and acute systemic safety profiles were mapped via SwissADME and ProTox-3.0 pipelines.

Pioglitazone demonstrated a high target affinity for the mitoNEET regulatory domain with a highly favorable Gibbs free energy score ($\Delta G = -31.8$ kJ/mol; binding constant 3.7×10^5), substantially outperforming Furosemide ($\Delta G = -26.4$ kJ/mol; binding constant 4.2×10^4). ADME screening confirmed strong drug-likeness, passive membrane permeability, and optimal lipophilicity ($\log P = 3.49$). Toxicological profiling classified pioglitazone under a safe acute operational envelope (Toxicity Class 4; $LD_{50} = 1000$ mg/kg), with low cardiotoxic or stress-response risks, though monitoring for potential hepatotoxicity (probability 0.70) remains necessary.

This research establishes a solid molecular foundation for repurposing pioglitazone in computational oncology. By binding stably to mitoNEET, pioglitazone is structurally positioned to alter mitochondrial bioenergetics and disrupt the vital ATP supply required for HKII-mediated cancer survival, justifying further advancement to *in vitro* validation assays.

Keywords: Drug Repurposing, Pioglitazone, Hexokinase II, MitoNEET (CISD1), Molecular Docking, Cancer Metabolism.